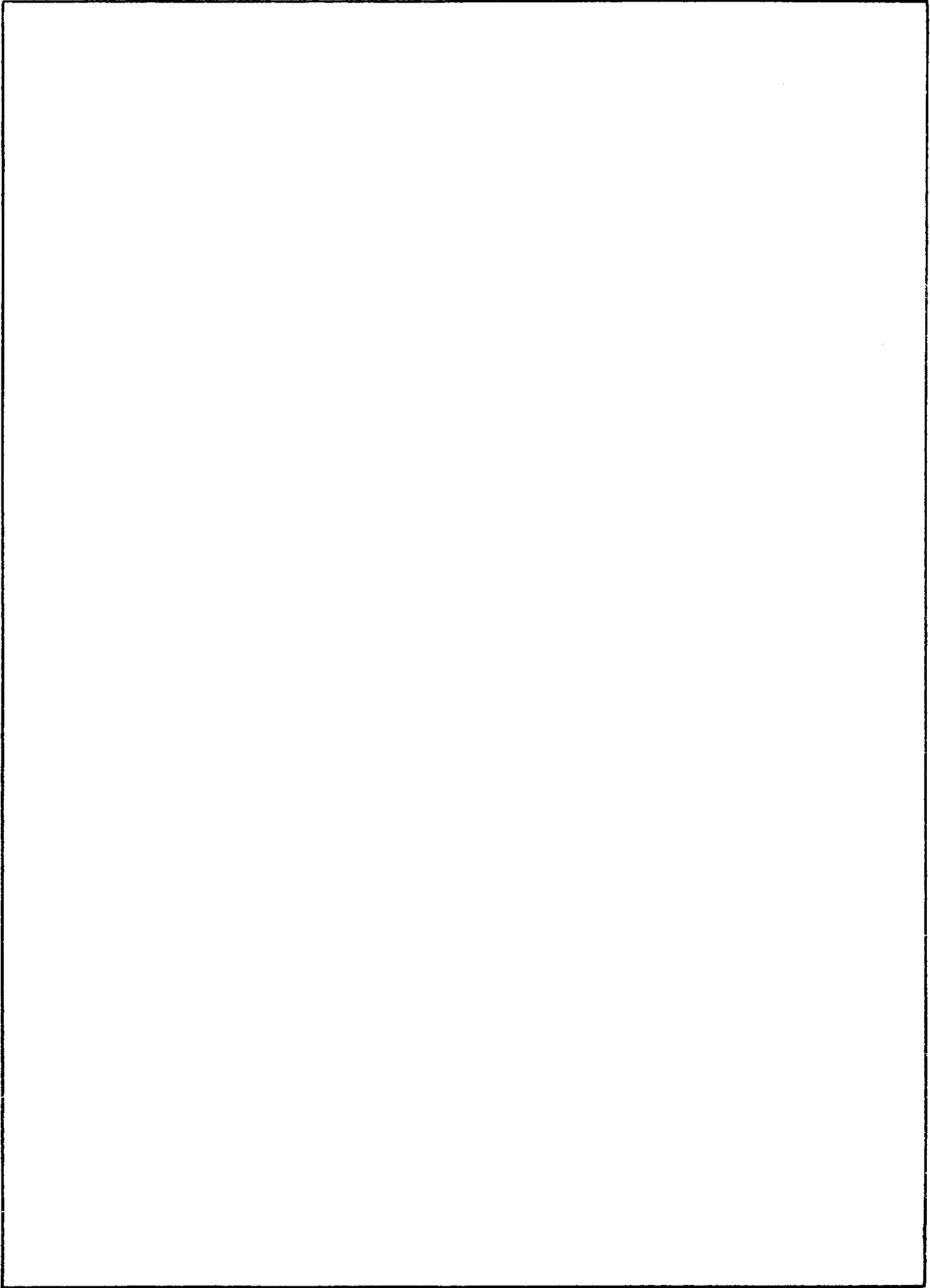


REPORT DOCUMENTATION PAGE		READ INSTRUCTIONS BEFORE COMPLETING FORM
1. REPORT NUMBER NRL Report 7851	2. GOVT ACCESSION NO.	3. RECIPIENT'S CATALOG NUMBER
4. TITLE (and Subtitle) AN ELASTO-CHEMICAL THEORY OF GRAIN BOUNDARIES		5. TYPE OF REPORT & PERIOD COVERED Final report on one phase of the NRL problem
		6. PERFORMING ORG. REPORT NUMBER
7. AUTHOR(s) R. A. Masumura and M. E. Glicksman		8. CONTRACT OR GRANT NUMBER(s)
9. PERFORMING ORGANIZATION NAME AND ADDRESS Naval Research Laboratory Washington, D.C. 20375		10. PROGRAM ELEMENT, PROJECT, TASK AREA & WORK UNIT NUMBERS NRL Problem M01-23 Proj. RR 022-01-46-5430
11. CONTROLLING OFFICE NAME AND ADDRESS Department of the Navy Office of Naval Research Arlington, Virginia 22217		12. REPORT DATE February 14, 1975
		13. NUMBER OF PAGES 44
14. MONITORING AGENCY NAME & ADDRESS (if different from Controlling Office)		15. SECURITY CLASS. (of this report) Unclassified
		15a. DECLASSIFICATION/DOWNGRADING SCHEDULE
16. DISTRIBUTION STATEMENT (of this Report) Approved for public release; distribution unlimited.		
17. DISTRIBUTION STATEMENT (of the abstract entered in Block 20, if different from Report)		
18. SUPPLEMENTARY NOTES		
19. KEY WORDS (Continue on reverse side if necessary and identify by block number) Crystals Grain boundary energy Dislocations Elasticity theory		
20. ABSTRACT (Continue on reverse side if necessary and identify by block number) An infinite periodic heterophase dislocation array is used as a model of a tilt boundary near the melting point of a crystalline solid. The elastic interaction among dislocations is included via a traction-free-core boundary condition. The elastic energy is coupled to the chemical energy from the core by an energy minimization scheme of the core radius. The theory yields the total grain boundary energy as function of tilt misorientation, which is found to compare favorably with experiments on bismuth.		



CONTENTS

INTRODUCTION	1
GRAIN BOUNDARY MODEL AND BOUNDARY CONDITIONS	3
ELASTIC SOLUTION	4
Review of Relevant Elasticity Theory	4
Elastic Potentials for Multivalued Displacements	6
Elastic Field and Rotational Properties of the Dislocation Array	9
Elastic Potentials for Single-Valued Displacements	11
Differential Boundary-Value Equation	11
Method of Solution	12
Mapping of a Periodic Strip	13
Transformation to Integral Equation	14
Elastic Energy	17
Transformation to the t plane	20
Numerical Solution	23
CORE ENERGY	25
GRAIN-BOUNDARY ENERGY	26
APPLICATION TO EXPERIMENT	30
SUMMARY	31
REFERENCES	32
APPENDIX A — Evaluation of the Complex Constants α and β ..	34
APPENDIX B — Elastic Field of a Single Isolated Edge Disloca- tion Obtained by Letting the Edge-Dislocation Spacing Approach Infinity in the Periodic Case	37
APPENDIX C — An Integral-Equation Approach to the Single Isolated Edge Dislocation With an Equilibrated Core	40

AN ELASTO-CHEMICAL THEORY OF GRAIN BOUNDARIES

INTRODUCTION

Grain boundaries significantly affect and control the physical properties of polycrystalline materials. For example, at temperatures near the melting point, grain boundaries play a dominant role in irreversible processes such as creep, diffusion, and sliding. To understand and exploit such phenomena, many models of grain boundaries have been proposed and analyzed in varying degrees of detail. However each is not without its inherent limitations which constrain its range of applicability in real materials.

The earliest attempt to quantify the structure of a crystalline grain boundary was Taylor's [1] study of plastic deformation by dislocation motion in metals. Taylor viewed a simple tilt boundary as an areal transition region between two symmetrically rotated lattices. (Taylor also considered the boundary to be composed of a geometrical series of regular steplike wedges joined at common lattice points—a possible precursor of the modern coincident-site lattice theory.) Later Burgers [2] considered the grain boundary between two crystalline lattices as a surface of misfit in the form of an array of edge dislocations. Using this concept, Burgers then determined the elastic stress components and rotational property of the array.

Read and Shockley [3] followed the formalism of Burgers and developed the well-known expression for the elastic energy of linear arrays of edge dislocations in an isotropic continuum. These investigators calculated the specific grain-boundary energy as a function of tilt misorientation. However, salient limitations exist in the theory of Read and Shockley. In their theory the singular behavior in the stress, strain, and energy-density fields at each dislocation in the boundary array was removed by postulating an inner "cutoff" radius r_0 . This maneuver provides mathematical tractability but prevents the theory from attaining a truly predictive status, because the radius r_0 must be determined from a grain-boundary-energy experiment. Also, the energetic contribution to the grain boundary energy from the cores of the dislocations in the array is neglected whenever a "cutoff" radius is employed; hence *all* interactions among the dislocations are per force ignored. This limitation clearly relegates the Read-Shockley dislocation model to small misorientation angles (to widely spaced arrays of dislocations), despite the apparent successes [4] achieved in "fitting" grain-boundary-energy data over large misorientations with the Read-Shockley equation.

Another approach used to describe crystalline boundaries is to consider the rotated crystal lattices as elastic *continua* with the common interfacial region described by discrete atomic locations. The interatomic potential between atoms in the interface yields the necessary boundary conditions to determine uniquely the longer-range elastic fields in the rotated continua. Van der Merwe [5] applied this method to describe simple tilt and twist boundaries using a sine force law (Peierls-Nabarro model). Fletcher and Adamson [6] then modified this scheme by taking the Fourier transform of the elastic displacements in

Note: Manuscript submitted November 29, 1974.

the continua and retaining only dominant terms. Their procedure leads to a variational formulation, which holds the number of parameters to a minimum. In all of these calculations where descriptions based on elastic continua and discrete atoms are mixed, the knowledge of the effective interatomic potential parameters is crucial but often lacking.

Hasson and Goux [7] employed yet another method to calculate the energies and structures of grain boundaries. They considered the interface as well as the rotated lattices *all* to consist of discrete atoms which interact via a Morse potential. The number of atoms and their configurations are varied to yield the lowest energy over a range of tilt misorientations. Such methods must be implemented numerically, using relaxation methods on a large high-speed computer; moreover, despite its sophistication, this approach generally excludes entropic contributions to the free energy and hence should be considered only as a calculation for 0 K. Unfortunately most experiments to determine grain boundary energies are performed at elevated temperatures (usually near the melting point) to facilitate a rapid approach to equilibrium; thus the correlation between the theoretical computations for 0 K and experiment is severely limited.

The structure of high-angle boundaries (misorientations greater than about 15°) has been systematically investigated at specific orientations by Ranganathan [8], Brandon [9], Bollmann [10], and Bishop and Chalmers [11]. Their main emphasis was to determine the geometrical relationships among lattice points in and adjacent to the boundary at so-called strong coincident sites, the calculation of boundary energy per se lying outside the scope of their lattice-geometric models.

By combining lattice-geometric concepts with dislocation-array models, the relative energy (only that portion arising from the defect array) can be obtained for very small misorientations about the lattice coincidence positions. The Burgers vector at the coincident sites can be determined as shown by Schober and Baluffi [12]. Unfortunately again, the reference energy level of the coincident site boundary to which the energy of the dislocation array is added cannot be calculated for temperatures greater than 0 K.

A modification of the earlier dislocation model for grain boundaries was proposed by Li [13], who attempted to account for effects arising from the dislocation cores. In his model Li considered first a single isolated edge dislocation with a circular core of radius r_0 that was traction free. He then superimposed the stress fields from these "hollow" dislocations in a periodic linear array to form a grain boundary. However in considering finite rotations (wherein the dislocations approach one another) the traction-free condition of the cores is altered, because the elastic interaction occurring among all the dislocations is ignored in the superposition method used by Li. To surmount this difficulty, Li proposed that the core shape was in some way dependent on the stresses acting near the core. Li's method yields a core radius which is larger than that calculated from the Read-Shockley model. Again, as in the Read-Shockley model, no truly predictive capability was achieved because of the entirely unknown nature of the parameter describing the core.

In a development parallel to that of Li, Glicksman and Vold [14] added a phenomenological core-energy term of thermodynamic origin and developed the concept of an equilibrated "heterophase" dislocation. This elasto-chemical approach yielded a predictive theory dependent only on known phenomenological variables and devoid of the usual unknown core parameter. Because this treatment formulates the elastic energy in a manner similar to that used by Li, the elastic boundary conditions at the core were again violated as the separation between dislocations decreased.

occurs away from the boundary, corresponding to the macroscopic tilt misorientation. Mathematically these conditions are

$$\left. \begin{array}{l} \sigma_{ij} \rightarrow 0 \\ |\nabla \times \mathbf{u}| \rightarrow \text{constant} \end{array} \right\}, \quad |x| < \infty, \quad |y| \rightarrow \infty, \quad (1)$$

where \mathbf{u} is the elastic displacement vector.

The analysis presented here will be separated into three steps. First the elastic energy of the system will be calculated using linear isotropic theory. Second the chemical energy from the core contribution will be formulated. Last the elastic and chemical energies will be minimized to yield via thermodynamics the equilibrium grain-boundary structure and energy.

ELASTIC SOLUTION

The discontinuity of displacement arising at each dislocation will produce stresses around every core boundary. However every core boundary is to be traction free. Therefore a linearly independent stress field with associated *single-valued* displacements is required to cancel the dislocation stresses at the core boundary. To distinguish these two elastic fields, those elastic quantities associated with the multivalued (dislocation) displacements will be denoted by either a subscript or superscript m , and those associated with the single-valued (core) displacements will be denoted by either a subscript or superscript s . The elastic field which maintains the dislocation cores traction free must also satisfy the following far-field conditions for a stress-free grain boundary:

$$\left. \begin{array}{l} \sigma_{ij}^{(s)} \rightarrow 0 \\ u_i^{(s)} \rightarrow 0 \\ |\nabla \times \mathbf{u}^{(s)}| \rightarrow 0 \end{array} \right\}, \quad |x| < \infty, \quad |y| \rightarrow \infty. \quad (2)$$

Review of Relevant Elasticity Theory

We digress here to review elements of linear isotropic elasticity theory which will be used heavily in this analysis. This approach uses the complex variable methods developed by Muskhelishvili [15], who introduced two complex elastic potentials $\phi(z)$ and $\psi(z)$, where $z = x + iy$, from which any two-dimensional elastic field can be obtained. The expressions relating $\phi(z)$ and $\psi(z)$ to the various elastic fields are derived by Muskhelishvili, and only the results will be presented here.

The stresses in a Cartesian xy coordinate system are given as

$$\sigma_{xx} + \sigma_{yy} = 2 \left[\phi'(z) + \overline{\phi'(z)} \right] \quad (3)$$

and

$$\sigma_{yy} - \sigma_{xx} + 2i\sigma_{xy} = 2 \left[z\phi''(z) + \psi'(z) \right], \quad (4)$$

where a prime denotes differentiation with respect to z and a bar denotes a complex conjugate. The displacements and forces between any two endpoints of an arc AB are

$$2G(u_x + iu_y)\Big|_A^B = \left[K\phi(z) - z\overline{\phi'(z)} - \psi(z) \right]\Big|_A^B, \quad (5)$$

$$(X + iY)\Big|_A^B = -i\left[\phi(z) + z\overline{\phi'(z)} + \overline{\psi(z)} \right]\Big|_A^B, \quad (6)$$

where u_x and u_y are the elastic displacements in the x and y directions respectively and X and Y are the corresponding components of the resultant force vector acting on AB in the x and y directions. The quantities G and K are material parameters: G is the shear modulus, and $K = 3 - 4\nu$, where ν is Poisson's ratio.

The general results of Muskhelishvili must be specialized when the elastic fields are periodic. Mikhlin [16] developed the necessary modifications of the forms for $\phi(z)$ and $\psi(z)$ for the periodic case. Mikhlin showed that by considering a periodic invariance in the stresses and displacements of the form

$$\left. \begin{aligned} \sigma_{ij}(x \pm nh, y) &= \sigma_{ij}(x, y) \\ u_i(x \pm nh, y) &= u_i(x, y) \end{aligned} \right\}, \quad n = \pm 1, \pm 2, \pm 3, \dots,$$

in Eqs. (3) through (5), $\phi(z)$ and $\psi(z)$ are modified as

$$\phi(z) = \phi_0(z); \quad \phi_0(z \pm nh) = \phi_0(z), \quad (7)$$

$$\psi(z) = \psi_0(z) - z\phi_0'(z); \quad \psi_0(z \pm nh) = \psi_0(z), \quad (8)$$

where the subscript zero denotes the periodic case. When Eqs. (7) and (8) are inserted into Eqs. (3) through (6), the elastic fields are periodic and are given as

$$\sigma_{xx} + \sigma_{yy} = 2\left[\phi_0'(z) + \overline{\phi_0'(z)} \right], \quad (9)$$

$$\sigma_{yy} - \sigma_{xx} + 2i\sigma_{xy} = 2\left[-2iy\phi_0''(z) + \psi_0(z) - \phi_0(z) \right], \quad (10)$$

$$2G(u_x + iu_y)\Big|_A^B = \left[K\phi_0(z) - 2iy\overline{\phi_0'(z)} - \psi_0(z) \right]\Big|_A^B, \quad (11)$$

and

$$X + iY\Big|_A^B = -i\left[\phi_0(z) + 2iy\overline{\phi_0'(z)} + \overline{\psi_0(z)} \right]\Big|_A^B. \quad (12)$$

Expressions (9) through (12) now permit us to proceed with the analysis of interacting grain boundary dislocations.

Elastic Potentials for Multivalued Displacements

The elastic potentials associated with periodic dislocations with multivalued displacements are obtained by generalizing the results of Muskhelishvili for a multiply connected elastic body. For a single dislocation at the origin of the xy coordinate system, the appropriate $\phi(z)$ and $\psi(z)$ are

$$\phi(z) = \alpha \ln z \quad (13)$$

and

$$\psi(z) = \beta \ln z, \quad (14)$$

where α and β are complex constants. For $2N + 1$ dislocations on the x axis and spaced a distance h apart, Eqs. (13) and (14) become

$$\phi = \sum_{-N}^N \alpha_n \ln (z + nh) \quad (15)$$

and

$$\psi = \sum_{-N}^N \beta_n \ln (z + nh). \quad (16)$$

Let us examine Eq. (15) first. Because of the $2N + 1$ identical dislocations we can set $\alpha = \alpha_n$ (complex constant) for all $|n| \leq N$. Then

$$\phi = \alpha \sum_{-N}^N \ln (z + nh),$$

which can be rewritten as

$$\phi = \alpha \ln \left[z \prod_1^N (z^2 - n^2 h^2) \right]$$

or

$$\phi = \alpha \ln \left\{ z \prod_1^N \left[1 - \left(\frac{z}{nh} \right)^2 \right] \right\} + \alpha \ln \prod_1^N (-n^2 h^2).$$

Let

$$f_N = \prod_1^N \left[1 - \left(\frac{z}{nh} \right)^2 \right]$$

and

$$C = \alpha \ln \prod_1^N (-n^2 h^2).$$

Since we have an infinite array of edge dislocations, we let $N \rightarrow \infty$ and recognize

$$f = \lim_{N \rightarrow \infty} f_N = z \prod_1^{\infty} \left[1 - \left(\frac{z}{nh} \right)^2 \right] = \sin \frac{\pi z}{h}.$$

But as $N \rightarrow \infty$, C increases without bound. However C has *no* functional dependence on z ; hence it has *no* effect on the stress or energy density distribution and may be interpreted as arising from an extraneous rigid-body translation. As such, the singular behavior of C as $N \rightarrow \infty$ is of no consequence. Thus for an infinite periodic array of edge dislocations the elastic potential ϕ becomes

$$\phi_{m0}(z) = \alpha \ln \sin \frac{\pi z}{h}. \quad (17)$$

Similarly for ψ we find

$$\psi_{m0}(z) = \beta \ln \sin \frac{\pi z}{h}. \quad (18)$$

The forms of these potentials, Eqs. (17) and (18), exhibit the proper periodicity to within a complex constant.

Complex elastic potentials of the form given by Eqs. (17) and (18) have been employed by other investigators for similar problems. Howland [17] and Schulz [18] used an analogous form in their investigations of stress distributions in plates containing an infinite array of circular holes. Their series method was handicapped by rather poor convergence and by the need for laborious matching of coefficients in the expansion. As a consequence they were able to solve specific problems only when the holes were widely separated from each other. Burgers [2], on the other hand, using mathematical techniques employed in hydrodynamics, was able to develop explicitly the necessary elastic field equations for a linear array of dislocations arbitrarily oriented in a crystal and obtained results similar to the multivalued potentials derived here.

The complex constants, α and β appearing in Eqs. (17) and (18) are evaluated from the conditions that each dislocation has a constant multivalued displacement vector and that a zero resultant force act on each dislocation. These conditions yield the two independent equations required to solve for α and β .

Mathematically a cut must be made at each dislocation to render the displacements single valued in the elastic body. On each side of the cut different values of the displacement are assigned. For the moment consider the zeroth dislocation, at the origin of the xy coordinate system (Fig. 2). We arbitrarily set $u_x = 0$ and $u_y = 0$ as $\xi \rightarrow -(3/2)\pi$ for any $r \geq r_0$ and set $u_x = 0$ and $u_y = b$ as $\xi \rightarrow \pi/2$ for any $r \geq r_0$. The quantity b is the discontinuity or jump in displacement: the magnitude of the dislocation's Burgers vector. Mathematically this is given as the line integral

$$\mathbf{b} = \oint \frac{\partial \mathbf{u}}{\partial s} ds, \quad (19)$$

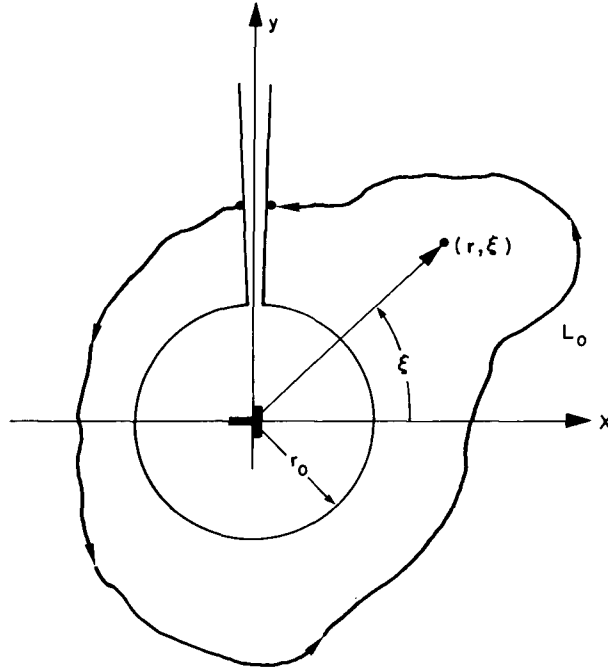


Fig. 2—The zeroth dislocation with a mathematical branch cut. L_0 is any contour enclosing the dislocation.

where $\mathbf{u} = (u_x, u_y)$, $\mathbf{b} = (0, b)$, and s is any closed path enclosing a grain boundary dislocation. Equation (19) has its complex analog given in terms of the complex potentials $\phi_{m0}(z)$ and $\psi_{m0}(z)$. Thus from Eq. (11) we find

$$2G \left(u_x^{(m)} + i u_y^{(m)} \right) \Big|_{L_0} = \left[K \phi_{m0}(z) - 2iy \overline{\phi'_{m0}(z)} - \overline{\psi_{m0}(z)} \right] \Big|_{L_0}, \quad (20)$$

where L_0 is any contour around a dislocation. When Eqs. (17) and (18) are inserted into Eq. (20) and evaluated (Appendix A gives the details), we obtain the result

$$2G(ib) = 2\pi i(K\alpha + \bar{\beta})$$

or

$$K\alpha + \bar{\beta} = \frac{Gb}{\pi}. \quad (21)$$

The condition of zero resultant force on the boundary dislocations requires that the tractions be zero on any contour enclosing a dislocation; thus Eq. (12) yields

$$(X + iY) \Big|_{L_0} = \left[\phi_{m0}(z) + 2iy \overline{\phi'_{m0}(z)} + \overline{\psi_{m0}(z)} \right] \Big|_{L_0} = 0.$$

When this equation is evaluated (as shown in Appendix A), the following result is obtained:

$$\alpha = \bar{\beta}. \quad (22)$$

Solving for α and $\bar{\beta}$ from Eqs. (21) and (22) yields

$$\alpha = \beta = \frac{Gb}{4\pi(1-\nu)},$$

which is a real constant and is identical to the energy factor for an *isolated* edge dislocation in an isotropic medium. In accord with the usual convention in the theory of dislocations, we define

$$E_0 \equiv \frac{Gb}{4\pi(1-\nu)}.$$

Then Eqs. (17) and (18) (the complex potentials) become

$$\phi_{m0}(z) = E_0 \ln \sin \frac{\pi z}{h} \quad (23)$$

and

$$\psi_{m0}(z) = E_0 \ln \sin \frac{\pi z}{h}. \quad (24)$$

Elastic Field and Rotational Properties of the Dislocation Array

The stresses and displacements for an infinite periodic array of edge dislocations can be determined by substituting Eqs. (23) and (24) into Eqs. (9) and (10). Some algebraic manipulation yields for the Cartesian stress components

$$\sigma_{xy}^{(m)} = \sigma_0 \frac{2\pi y}{h} \left(1 - \cos \frac{2\pi x}{h} \cosh \frac{2\pi y}{h} \right), \quad (25)$$

$$\sigma_{xx}^{(m)} = \sigma_0 \sin \frac{2\pi x}{h} \left(\cosh \frac{2\pi y}{h} - \cos \frac{2\pi x}{h} - \frac{2\pi y}{h} \sinh \frac{2\pi y}{h} \right), \quad (26)$$

and

$$\sigma_{yy}^{(m)} = \sigma_0 \sin \frac{2\pi x}{h} \left(\cosh \frac{2\pi y}{h} - \cos \frac{2\pi x}{h} + \frac{2\pi y}{h} \sinh \frac{2\pi y}{h} \right), \quad (27)$$

where

$$\sigma_0 = \frac{2E_0 \frac{\pi}{h}}{\left(\cosh \frac{2\pi y}{h} - \cos \frac{2\pi x}{h} \right)^2}.$$

The stresses, $\sigma_{ij}^{(m)}$ are invariant under a translation $x = x \pm ph$, $p = 0, 1, 2, 3, \dots$, and decay away from the boundary plane ($\sigma_{ij}^{(m)} \rightarrow 0$ for $|x| \rightarrow \infty$, $|y| \rightarrow \infty$). Equations (25) through (27) are similar in form to those derived by other methods by Li [13] and by Hirth and Lothe [19] for a dislocation array along the y axis.

The Cartesian components of the displacement are

$$u_x^{(m)} = \frac{E_0}{2G} \left[(K-1) \ln M + \frac{\pi y}{h} \frac{\sinh \frac{2\pi y}{h}}{M^2} \right] \quad (28)$$

and

$$u_y^{(m)} = \frac{E_0}{2G} \left[(K+1) \tan^{-1} \left(\frac{\tanh \frac{\pi y}{h}}{\tan \frac{\pi x}{h}} \right) - \frac{\pi y}{h} \frac{\sinh \frac{2\pi y}{h}}{M^2} \right], \quad (29)$$

where

$$M^2 = \sinh^2 \frac{\pi y}{h} + \sin^2 \frac{\pi x}{h}.$$

Burgers [2] developed expressions similar to Eqs. (28) and (29), except that his coordinate system is rotated by $\pi/2$ from the coordinate system used in this analysis. The elastic fields of the single isolated edge dislocation can of course be recaptured by letting $h \rightarrow \infty$ in Eqs. (25) through (29), as shown in Appendix B.

The rotation of the elastic body is given as

$$\omega = \frac{1}{2} |\nabla \times \mathbf{u}|$$

which is the antisymmetric part of the general deformation tensor. Muskhelishvili has shown [15, p. 127] that the rotation can be written in terms of the complex potential $\phi_{m0}(z)$ as

$$\omega = \frac{K+1}{2G} \operatorname{Im} \left[\phi'_{m0}(z) \right],$$

where $\operatorname{Im} [\dots]$ denotes the imaginary part. Substituting for $\phi_{m0}(z)$ from Eq. (23) yields the rotation field

$$\omega(x, y) = \frac{b}{2h} \frac{\sinh \frac{2\pi y}{h}}{\left[\cosh \frac{2\pi y}{h} - \cos \frac{2\pi x}{h} \right]},$$

which, as $y \rightarrow \pm\infty$, yields the "strain-free" (constant) rotations far from the boundary plane:

$$\omega_+ = \lim_{y \rightarrow +\infty} \omega = \frac{-b}{2h}$$

and

$$\omega_- = \lim_{y \rightarrow -\infty} \omega = \frac{b}{2h}.$$

This result is consistent with the boundary conditions of Eq. (1). The total tilt misorientation θ between the two grains is therefore

$$\theta = |\omega_+ - \omega_-| = \frac{b}{h}, \quad (30)$$

which agrees with the result of Burgers [2] and Nabarro [20] who used a continuous distribution of dislocations to simulate an infinite array. *The rotational behavior of the dislocation array was developed without any consideration of the latticelike nature of the rotated crystals.* Equation (30) devolves entirely from the theory of elasticity without lattice geometrical considerations. Also Eq. (30) provides an operational definition of the Burgers vector of tilt boundary dislocations: The Burgers vector remains normal to the boundary plane and is of magnitude θh , where both θ and h may be obtained via *independent* experiments.

Elastic Potentials for Single-Valued Displacements

The boundary conditions for our grain boundary model require traction-free dislocation cores. The dislocation stresses arising from the multivalued displacements are canceled along the core boundary by a *linearly independent* stress field possessing single-valued displacements. Thus a second set of complex potentials $\phi_{s0}(z)$ and $\psi_{s0}(z)$ are required from which the compatible single-valued elastic fields can be determined.

Differential Boundary-Value Equation

For the moment let us consider one hole in an infinite elastic medium. Mathematically, as indicated in Fig. 3, we have an infinite region S bounded by a simple internal contour L , where n is the normal to L at point z . Let $X_n(z)$ and $Y_n(z)$ be the vector components of the tractions applied on L . From the relationship between the boundary tractions and the real Airy stress function, Muskhelishvili showed [15, p. 145] that the boundary condition in terms of complex potentials is given as

$$\phi_a(z) + \overline{\phi'_a(z)} + \overline{\psi_a(z)} = f_1 + if_2 \quad (31)$$

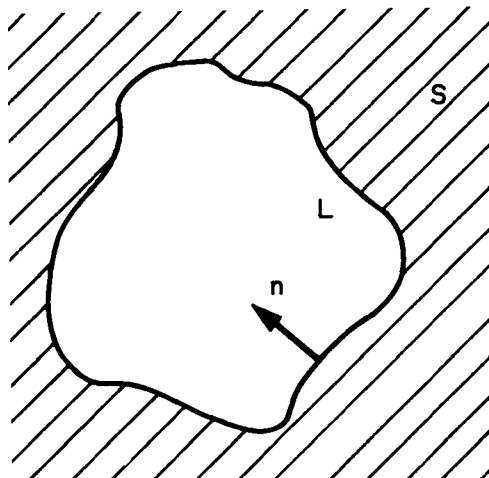


Fig. 3—An arbitrarily shaped hole L in an infinite medium S

for all $z \in L$. The subscript a refers to this special case, and f_1 and f_2 are functions of the tractions $X_n(z)$ and $Y_n(z)$. Equation (31) is similar to Eq. (6).

Generalizing this special situation to the periodic array in the same manner as in the section titled "Review of Relevant Elasticity Theory," the governing differential equation becomes

$$\phi_0(z) + 2iy\overline{\phi_0'(z)} + \overline{\psi_0(z)} = F_1 + iF_2 + \text{complex constant}, \quad (32)$$

where z is any point on any dislocation core boundary of the array and F_1 and F_2 are functions of the applied tractions. The complex potentials are the sum of the contributions accounting for the multivalued and single-valued displacements:

$$\phi_0(z) = \phi_{s0}(z) + \phi_{m0}(z)$$

and

$$\psi_0(z) = \psi_{s0}(z) + \psi_{m0}(z).$$

When the boundary is traction free, then

$$F_1 = F_2 = 0,$$

and Eq. (32) becomes

$$\phi_{s0}(z) + 2iy\overline{\phi_{s0}'(z)} + \overline{\psi_{s0}(z)} = F(z) + \text{complex constant},$$

where

$$F(z) = -\left[\phi_{m0}(z) + 2iy\overline{\phi_{m0}'(z)} + \overline{\psi_{m0}(z)}\right]. \quad (33)$$

If we have periodicity in the "single-valued" potentials, that is,

$$\phi_{s0}(z) = \phi_{s0}(z \pm nh) \quad \text{and} \quad \psi_{s0}(z) = \psi_{s0}(z \pm nh), \quad n = 1, 2, 3, \dots,$$

then the constant must be the same for each hole and hence can be set equal to zero. Therefore the differential equation to be solved is

$$\phi_{s0}(z) + 2iy\overline{\phi_{s0}'(z)} + \overline{\psi_{s0}(z)} = F(z), \quad (34)$$

where $F(z)$ can be evaluated explicitly, since $\phi_{m0}(z)$ and $\psi_{m0}(z)$ are now known. At this point the problem has been reduced to an infinite set of periodic holes, each subjected to identical (zero) tractions. The elastic field obtained from $\phi_{s0}(z)$ and $\psi_{s0}(z)$ must also satisfy the far-field conditions given in Eq. (2).

Method of Solution

Equation (34) could be solved as given, but this would require an infinite set of differential equations, one for each hole. A more tractable scheme was developed by Mikhlín [16] in which each periodic unit or strip is conformally and identically mapped into another plane. In this new plane the resulting differential equation is converted via

the mapping transformations into a complex Fredholm integral equation of the second kind which can be easily solved numerically. The solution of the integral equation yields values of the complex potentials along a closed contour. The potentials anywhere else in the plane can then be found by application of Cauchy's formulas. (The case of the single or isolated dislocation with a traction-free core in an infinite medium can also be analyzed by the integral equation approach, as shown in Appendix C.)

Our objective now is to determine the elastic energy contained in one of the periodic strips. It will be shown in later sections that this energy can be formulated in terms of the single- and multivalued complex potentials.

Mapping of a Periodic Strip

Mikhlin's [16] method involves mapping a periodic region in the z plane ($z = x + iy$) to the t plane ($t = u + iv$) by the transformation

$$t = e^{2\pi iz/h} . \quad (35)$$

This relation takes any strip $(h/2)(2n - 1) \leq x \leq (h/2)(2n + 1)$, $n = 0, \pm 1, \pm 2, \dots$, and $|y| \leq \infty$ and maps it into the *entire* t plane. Therefore only one differential equation is required for the complete determination of elastic potentials in the t plane.

Let the zeroth strip (the one containing the origin of the xy axes) be mapped into the t plane via Mikhlin's transformation. The circle $z = r_0 e^{i\xi}$ in the z plane becomes in the t plane

$$\tau = \exp(2\pi i \mu e^{i\xi}), \quad 0 \leq \xi \leq 2\pi , \quad (36)$$

where τ represents points on the kidney-shaped boundary in the t plane (Fig. 4), $\mu = r_0/h$, in which h is the width of the strip (h is also the spacing between dislocations), and ξ is the polar angle in the z plane. As shown in Fig. 4, L is the contour of the kidney-shaped hole in the t plane; S^+ is the region inside this hole, and S^- is the surrounding elastic medium.

The differential equation to be solved, Eq. (34), can now be transformed into the t plane. Let

$$\Phi_{s0}(\tau) \equiv \phi_{s0}[z(\tau)] \quad \text{and} \quad \Psi_{s0}(\tau) \equiv \psi_{s0}[z(\tau)] .$$

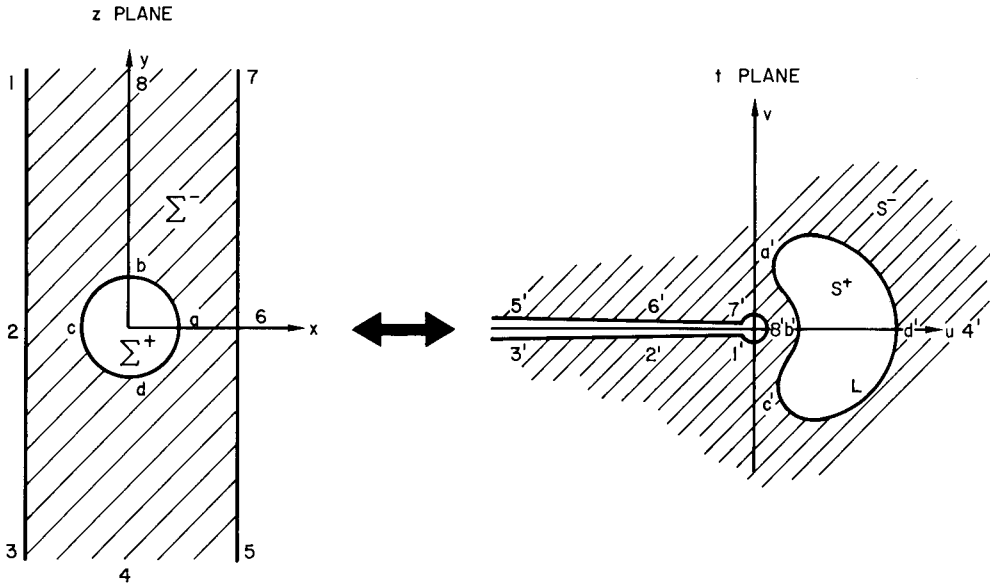
Using the chain rule for differentiation, we have

$$\frac{\partial \phi_{s0}}{\partial z} = \frac{\partial \Phi_{s0}}{\partial \tau} \frac{\partial \tau}{\partial z} ,$$

where $\partial \tau / \partial z$ can be determined from Eq. (35). Thus Eq. (34) becomes

$$\Phi_{s0}(\tau) - 2\bar{\tau} \ln |\tau| \overline{\Phi'_{s0}(\tau)} + \overline{\Psi_{s0}(\tau)} = F(\tau) , \quad (37)$$

where $F(\tau) = F[z(\tau)]$, as given by Eq. (33), and the prime means differentiation with respect to τ .


 Fig. 4—Mapping of the zeroth strip in the z plane into the t plane

Transformation to Integral Equation

Equation (37) can be converted to a complex Fredholm integral equation of the second kind as shown by Mikhlin. First we take the complex conjugate of (37) and rewrite it as

$$\Psi_{s_0}(\tau) = \overline{F(\tau)} - \overline{\Phi_{s_0}(\tau)} + 2\tau \ln |\tau| \Phi'_{s_0}(\tau). \quad (38)$$

If $\Psi_{s_0}(\tau)$ is to be the boundary value of some function holomorphic in S^- and continuous in $S^- + L$ (including $t = \infty$), then [15, p. 285, Theorem II]

$$\frac{1}{2\pi i} \int_L \frac{\Psi_{s_0}(\tau)}{\tau - t'} d\tau = \frac{1}{2\pi i} \int_L \frac{\overline{F(\tau)} - \overline{\Phi_{s_0}(\tau)} + 2\tau \ln |\tau| \Phi'_{s_0}(\tau)}{\tau - t'} d\tau = \Psi_{s_0}(\infty) \quad (39)$$

for any arbitrary point $t' \in S^+$ (a point inside the hole), where $\Psi_{s_0}(\infty)$ is a constant. Thus $\Psi_{s_0}(\tau)$ and $\Phi_{s_0}(\tau)$ can be determined to within a constant. To fix this constant, let $\Psi_{s_0}(\infty) = 0$; then Eq. (39) becomes

$$\frac{1}{2\pi i} \int_L \frac{\Phi_{s_0}(\tau)}{\tau - t'} d\tau - \frac{1}{2\pi i} \int_L \frac{2\tau \ln |\tau| \Phi'_{s_0}(\tau)}{\tau - t'} d\tau = A(t'), \quad (40)$$

where

$$A(t') = \frac{1}{2\pi i} \int_L \frac{\overline{F(\tau)}}{\tau - t'} d\tau. \quad (41)$$

Once Eq. (40) (or its equivalent form) has been solved for $\Phi_{s_0}(\tau)$, then $\Psi_{s_0}(\tau)$ can be calculated from Eq. (38).

Since $\Phi_{s0}(t)$ and $\Psi_{s0}(t)$ are holomorphic in S^- and continuous in $S^- + L$, they are related to $\Phi_{s0}(\tau)$ and $\Psi_{s0}(\tau)$ by Cauchy's "outside" formula [15, p. 268, Eq. 70.1] (for the infinite region S^-):

$$\Phi_{s0}(t) = -\frac{1}{2\pi i} \int_L \frac{\Phi_{s0}(\tau)}{\tau - t} d\tau + \Phi_{s0}(\infty) \quad (42)$$

and

$$\Psi_{s0}(t) = -\frac{1}{2\pi i} \int_L \frac{\Psi_{s0}(\tau)}{\tau - t} d\tau \quad (43)$$

(recalling that $\Psi_{s0}(\infty) = 0$), where

$$\Phi_{s0}(\infty) = \frac{1}{2\pi i} \int_L \frac{\Phi_{s0}(\tau)}{\tau - t'} d\tau, \quad t' \in S^+. \quad (44)$$

Equation (40) can be converted to a Fredholm equation of the second kind. Since $\Phi_{s0}(t)$ is regular in S^- , and since $t' \in S^+$, by Eq. (42)

$$\frac{1}{2\pi i} \int_L \frac{\Phi_{s0}(\tau)}{\tau - t'} d\tau = \Phi_{s0}(\infty) = \text{constant}.$$

Thus

$$\frac{1}{2\pi i} \frac{\partial}{\partial t'} [\Phi_{s0}(\infty)] = \frac{1}{2\pi i} \int_L \frac{\Phi_{s0}(\tau)}{(\tau - t')^2} d\tau = 0,$$

which, after integration by parts, becomes

$$\frac{1}{2\pi i} \left[-\frac{\Phi_{s0}(\tau)}{\tau - t'} \right]_L + \frac{1}{2\pi i} \int_L \frac{\Phi'_{s0}(\tau)}{\tau - t'} d\tau = 0.$$

But

$$\frac{\Phi_{s0}(\tau)}{\tau - t'} \Big|_L = 0;$$

thus

$$\frac{1}{2\pi i} \int_L \frac{\Phi'_{s0}(\tau)}{\tau - t'} d\tau = 0. \quad (45)$$

We multiply (45) by $2t' \ln |t'|$, with again $t' \in S^+$; then

$$\frac{1}{2\pi i} \int_L \frac{2t' \ln |t'| \Phi'_{s0}(\tau)}{\tau - t'} d\tau = 0. \quad (46)$$

We let c be a fixed point inside L (c is arbitrary, and for convenience we choose $c \equiv 1$); then

$$\frac{1}{2\pi i} \int_L \frac{\Phi_{s_0}(\tau)}{\tau - t'} d\tau - \frac{1}{2\pi i} \int_L \frac{\overline{\Phi_{s_0}(\tau)}}{\bar{\tau} - \bar{t}'} d\bar{\tau} = 0. \quad (47)$$

Adding Eq. (46) and the conjugate of Eq. (47) to Eq. (40), we get

$$\begin{aligned} & \frac{1}{2\pi i} \int_L \frac{\overline{\Phi_{s_0}(\tau)}}{\bar{\tau} - \bar{t}'} d\bar{\tau} - \frac{1}{2\pi i} \int_L \frac{2\tau \ln |\tau| \Phi'_{s_0}(\tau)}{\tau - t'} d\tau \\ & + \frac{1}{2\pi i} \int_L \frac{2t' \ln |t'| \Phi'_{s_0}(\tau)}{\tau - t'} d\tau + \frac{1}{2\pi i} \int_L \frac{\overline{\Phi_{s_0}(\tau)}}{\bar{\tau} - \bar{t}'} d\bar{\tau} \\ & - \frac{1}{2\pi i} \int_L \frac{\overline{\Phi_{s_0}(\tau)}}{\bar{\tau} - \bar{c}} d\bar{\tau} = A(t'), \quad t' \in S^+. \end{aligned} \quad (48)$$

In Eq. (48) we would like to recast $\Phi'_{s_0}(\tau)$ in terms of $\Phi_{s_0}(\tau)$. Then integrating by parts, where $g(\tau, t')$ is any regular function, we get

$$\int_L g(\tau, t') \Phi'_{s_0}(\tau) d\tau = \Phi_{s_0}(\tau) g(\tau, t') \Big|_L - \int_L \Phi_{s_0}(\tau) \frac{\partial g}{\partial \tau} d\tau.$$

But

$$\Phi_{s_0}(\tau) g(\tau, t') \Big|_L = 0;$$

thus

$$\int_L g(\tau, t') \Phi'_{s_0}(\tau) d\tau = - \int_L \Phi_{s_0}(\tau) \frac{\partial g}{\partial \tau} d\tau. \quad (49)$$

Using (49) in (48), we get

$$\begin{aligned} & \frac{1}{2\pi i} \int_L \frac{\overline{\Phi_{s_0}(\tau)}}{\bar{\tau} - \bar{t}'} d\bar{\tau} - \frac{1}{2\pi i} \int_L \frac{\Phi_{s_0}(\tau)}{\tau - c} d\tau + \frac{1}{\pi i} \int_L \Phi_{s_0}(\tau) d \left(\frac{\tau \ln |\tau| - t' \ln |t'|}{\tau - t'} \right) \\ & + \frac{1}{2\pi i} \int_L \frac{\overline{\Phi_{s_0}(\tau)}}{\bar{\tau} - \bar{c}} d\bar{\tau} = A(t'). \end{aligned} \quad (50)$$

We let $t' \rightarrow \tau_0$, where $\tau_0 \in L$, and let f denote the principal value of an integral; then from Plemelj's formula [15, p. 262]

$$\frac{1}{2\pi i} \int_L \frac{f(\tau) d\tau}{\tau - t'} = \frac{1}{2} f(\tau_0) + \frac{1}{2\pi i} \int \frac{f(\tau) d\tau}{\tau - t_0},$$

provided $f(\tau)$ is Hölder continuous in the neighborhood of τ_0 of L . Then (50) becomes

$$\begin{aligned} & \overline{\Phi_{s0}(\tau_0)} - \frac{1}{2\pi i} \int \frac{\overline{\Phi_{s0}(\tau)}}{\bar{\tau} - \bar{\tau}_0} d\bar{\tau} + \frac{1}{2\pi i} \int \frac{\overline{\Phi_{s0}(\tau)}}{\bar{\tau} - \bar{\tau}_0} d\tau \\ & + \frac{1}{\pi i} \int \Phi_{s0}(\tau) d\left(\frac{\tau \ln |\tau| - \tau_0 \ln |\tau_0|}{\tau - \tau_0}\right) + \frac{1}{2\pi i} \int \frac{\Phi(\tau)}{\bar{\tau} - \bar{c}} d\bar{\tau} = A(\tau_0). \end{aligned} \quad (51)$$

Equation (51) is not solvable, because the homogeneous equation has a nontrivial solution (Fredholm's alternative theorem). Savin [21] and Sherman [22] have pointed out that by adding to the left-hand side of (51) the term

$$\frac{i}{2\pi} \overline{\ln \tau_0} \operatorname{Re} \left[\int \frac{\Phi_{s0}(\tau)}{(\tau - c)^2} d\tau \right] = 0,$$

the homogeneous solution becomes the trivial one and therefore, by Fredholm's alternative theorem, a solution exists for the inhomogeneous equation. The integral equation now has the form

$$\begin{aligned} & \overline{\Phi_{s0}(\tau_0)} + \frac{1}{2\pi i} \int \Phi_{s0}(\tau) d\left(\ln \frac{\tau - \tau_0}{\bar{\tau} - \bar{\tau}_0}\right) \\ & + \frac{1}{\pi i} \int \Phi_{s0}(\tau) d\left(\frac{\tau \ln |\tau| - \tau_0 \ln |\tau_0|}{\tau - \tau_0}\right) \\ & + \frac{i}{2\pi} \ln \tau_0 \operatorname{Re} \left[\int_L \frac{\Phi(\tau)}{\tau - c} d\tau \right] + \frac{1}{2\pi i} \int_L \frac{\overline{\Phi(\tau)}}{\bar{\tau} - \bar{c}} d\bar{\tau} = A(\tau_0). \end{aligned} \quad (52)$$

The inhomogeneous term is expressed as

$$A(\tau_0) = \frac{1}{2\pi i} \int_{t' \rightarrow \tau_0} \frac{\overline{F(\tau)}}{\tau - t'} d\tau = \frac{\overline{F(\tau_0)}}{2} + \frac{1}{2\pi i} \int \frac{\overline{F(\tau)}}{\tau - \tau_0} d\tau, \quad (53)$$

since $\overline{F(\tau)}$ is Hölder continuous on L . Equation (52) is now in a form amenable for numerical computation; its solution will be discussed later.

Elastic Energy

The solution to Eq. (52) yields $\Phi_{s0}(\tau)$ along the boundary L ; hence one can determine $\Psi_{s0}(\tau)$. From these potentials, $\Phi_{s0}(t)$ and $\Psi_{s0}(t)$ can be obtained for any $t \in S^-$. We will now develop expressions for the elastic energy contained in any strip in terms of the complex potentials, first in the z plane and later in the t plane.

The elastic energy of a strip in the z plane is given by Clapeyron's theorem [23] as

$$E_{\text{elas}} = \frac{1}{2} \int_L \nu T_{ij} u_j dL, \quad (54)$$

where $T_{ij}^\nu = \sigma_{ji}\nu_i$ is the i th component of the traction acting on surface L with normal ν and direction cosines ν_j . The elastic field quantities σ_{ij} and u_i in Eq. (54) are the sum of the single and multivalued contributions for the stress and displacement respectively, that is,

$$\sigma_{ij} = \sigma_{ij}^{(m)} + \sigma_{ij}^{(s)} \quad \text{and} \quad u_i = u_i^{(m)} + u_i^{(s)}.$$

Because u_i is in part the multivalued displacement from the dislocations, a branch cut is required when evaluating the Clapeyron contour integral, Eq. (54), as illustrated in Fig. 5.

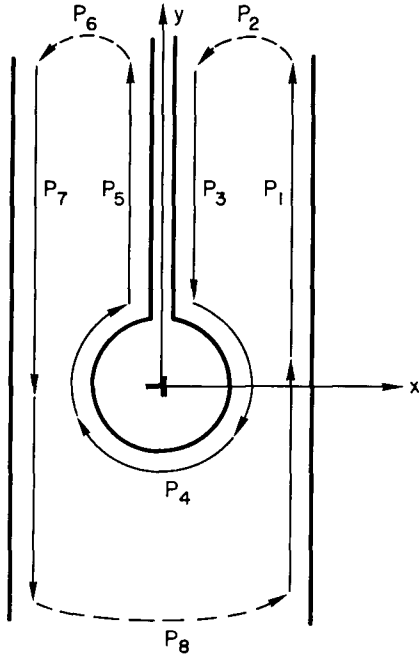


Fig. 5—Path of integration for elastic energy in the z plane. The total closed path is $P = P_1 + P_2 + \dots + P_7 + P_8$.

The elastic energy is the sum of eight integrals evaluated on P_1, P_2, \dots, P_8 . Let us examine the contributions from P_3 and P_5 along each side of the branch cut. Applying Eq. (54), we have

$$E_{\text{elas}}^{P_3} = -\frac{1}{2} \int_{r_0}^{\infty} W|_{x=0^+} dy$$

and

$$E_{\text{elas}}^{P_5} = \frac{1}{2} \int_{r_0}^{\infty} W|_{x=0^-} dy$$

or

$$E_{\text{elas}}^{P_3+P_5} = \frac{1}{2} \int_{r_0}^{\infty} (W|_{x=0^-} - W|_{x=0^+}) dy, \quad (55)$$

where $W = \sigma_{xx}u_x + \sigma_{xy}u_y$. The integrand of Eq. (55) can be rewritten as

$$\Delta W = \sigma_{xx}u_x \Big|_{x=0^+}^{x=0^-} + \sigma_{xy}u_y \Big|_{x=0^+}^{x=0^-} \quad (56)$$

However the only term in Eq. (56) which yields a nonzero contribution is

$$\Delta W = \sigma_{xy}(x, y)u_y(x, y) \Big|_{x=0^+}^{x=0^-} = \sigma_{xy}(0, y)\Delta u_y^{(m)}$$

But as shown in Eq. (19)

$$\Delta u_y^{(m)} = b.$$

Thus

$$E_{\text{elas}}^{P_3+P_5} = \frac{b}{2} \int_{r_0}^{\infty} \sigma_{xy}(0, y) dy,$$

where $\sigma_{xy}(0, y)$ is the sum of the single and multivalued shear stresses. The contributions from P_1 and P_7 are in a similar manner

$$E_{\text{elas}}^{P_1+P_7} = \frac{1}{2} \int_{-\infty}^{+\infty} (W|_{x=h/2} - W|_{x=-h/2}) dy, \quad (57)$$

where $W = \sigma_{xx}u_x + \sigma_{xy}u_y$. Again the integrand of (57) can be written as

$$\Delta W = \sigma_{xx}u_x \Big|_{-h/2}^{h/2} + \sigma_{xy}u_y \Big|_{-h/2}^{h/2} \quad (58)$$

Because of the periodicity of the elastic fields,

$$\sigma_{ij}(h/2, y) = \sigma_{ij}(-h/2, y)$$

and

$$u_i(h/2, y) = u_i(-h/2, y),$$

and Eq. (58) becomes $\Delta W = 0$. Hence $E_{\text{elas}}^{P_1+P_7} = 0$. The stress boundary conditions at P_4 demand that $\sigma_{rr} = \sigma_{r\xi} = 0$ for $r = r_0$. Hence $E_{\text{elas}}^{P_4} = 0$.

The integrals from P_2 , P_6 , and P_8 for $y \rightarrow \pm\infty$, $|x| \leq h/2$, are zero due to the stresses vanishing. In this far-field limit, $\sigma_{ij}^{(m)}$ and $u_i^{(m)}$ assume the forms

$$\sigma_{xy}^{(m)} \sim e^{-4\pi|y|/h},$$

$$\sigma_{xx}^{(m)} \sim \sin \frac{2\pi x}{h} e^{-2\pi y/h},$$

$$u_x^{(m)} \sim y,$$

and

$$u_y^{(m)} \sim \text{constant.}$$

From Eq. (2) the single-valued terms must vanish in the far field. Thus, because of the exponential decay of $\sigma_{ij}^{(m)}$ as $y \rightarrow \pm\infty$, it follows that $E_{\text{elas}}^{P_2} = E_{\text{elas}}^{P_6} = E_{\text{elas}}^{P_8} = 0$. Hence, as one might expect, the elastic energy of a strip is

$$E_{\text{elas}} = E_{\text{elas}}^{P_3+P_5} = \frac{b}{2} \int_{r_0}^{\infty} \sigma_{xy}(0, y) dy. \quad (59)$$

Transformation to the t Plane

The elastic energy, Eq. (59), is expressed in terms of variables in the z plane. Since the single-valued potentials are determined in the t plane, it is convenient to transform Eq. (59) to the t plane. Again each strip including the branch cut is mapped from the z plane into the entire t plane by the transformation given by Eq. (35). As shown in Fig. 6, only segments P'_3 and P'_5 of the t -plane contour contribute to the Clapeyron integral.

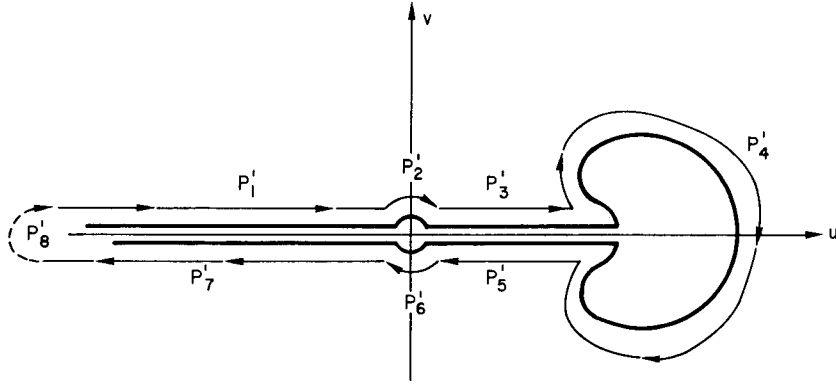


Fig. 6—Path of integration in the t plane

Separating Eq. (35) into its real and imaginary parts yields

$$u(x, y) = \cos \frac{2\pi x}{h} e^{-2\pi y/h}$$

and

$$v(x, y) = \sin \frac{2\pi x}{h} e^{-2\pi y/h},$$

and inserting these into Eq. (59) when $x = 0$ and $y \geq r_0$ yields

$$E_{\text{elas}} = \frac{b}{2} \int_{\epsilon \rightarrow 0}^{u_0} \frac{h}{2\pi} S_{xy}(u, 0) \frac{du}{u}, \quad (60)$$

where $S_{xy}(u, 0)$ is $\sigma_{xy}(0, y)$ transformed into the t plane. The upper limit in Eq. (60) is

$$u_0 = e^{-2\pi\mu},$$

where $\mu = r_0/h$; hence E_{elas} is a function of μ only.

$S_{xy}(u, 0)$ can be determined through Eq. (10), which relates the shear stress to the complex potentials in the z plane. Transforming Eq. (10) into the t plane using Eq. (35), using the chain-rule relationships

$$\frac{\partial \phi}{\partial z} = \frac{\partial \Phi}{\partial t} \frac{\partial t}{\partial z}$$

and

$$\frac{\partial^2 \phi}{\partial z^2} = \frac{\partial^2 \Phi}{\partial t^2} \left(\frac{\partial t}{\partial z} \right)^2 + \frac{\partial \Phi}{\partial t} \frac{\partial^2 t}{\partial z^2}$$

and then inserting these results into Eq. (60) gives the elastic energy as

$$E_{\text{elas}} = \frac{b}{2} \int_{\epsilon \rightarrow 0}^{u_0} \left[\Psi'_{\text{Re}} - \Phi'_{\text{Re}} - 2 \ln u (\Phi''_{\text{Re}} u + \Phi'_{\text{Re}}) \right] du, \quad (61)$$

where the prime denotes differentiation with respect to u and the subscript Re means the real part. Equation (61) can be integrated by parts to yield

$$E_{\text{elas}} = \frac{b}{2} \left(\Psi_{\text{Re}} + \Phi_{\text{Re}} - 2u \ln u \Phi'_{\text{Re}} \right) \Big|_{\epsilon \rightarrow 0}^{u_0}.$$

However, if we recall that

$$\Phi = \Phi_{s0} + \Phi_{m0}$$

and

$$\Psi = \Psi_{s0} + \Psi_{m0},$$

then the expression for elastic energy may be written as

$$E_{\text{elas}} = E_{\text{elas}}^{(m)} + E_{\text{elas}}^{(s)},$$

where

$$E_{\text{elas}}^{(s)} = \frac{b}{2} \left(\Psi_{\text{Re},s0} + \Phi_{\text{Re},s0} - 2u \ln u \Phi'_{\text{Re},s0} \right) \Big|_{\epsilon \rightarrow 0}^{u_0} \quad (62)$$

and

$$E_{\text{elas}}^{(m)} = \frac{b}{2} \left(\Psi_{\text{Re},m0} + \Phi_{\text{Re},m0} - 2u \ln u \Phi'_{\text{Re},m0} \right) \Big|_{\epsilon \rightarrow 0}^{u_0}. \quad (63)$$

Equation (63) can be evaluated immediately, since ϕ_{m0} and ψ_{m0} are known (Eqs. (23) and (24)). Using the transformation given by Eq. (35), Eq. (63) becomes

$$E_{\text{elas}}^{(m)}(\mu) = E_0 b [\pi \mu \coth \pi \mu - \ln(2 \sinh \pi \mu)], \quad (64)$$

which is equivalent to the form derived by Read and Shockley [3], Li [13], and Hirth and Lothe [19]. This is to be expected, as $E_{\text{elas}}^{(m)}(\mu)$ is the elastic energy of the edge dislocation array without any consideration of the core boundary conditions, that is, *without any elastic interactions*.

The single-valued energy, Eq. (62), may be simplified further by examining its behavior as $u \rightarrow 0$ (or $\epsilon \rightarrow 0$). Points near the origin in the t plane are mapped into the z plane as points $y \rightarrow \infty$. In the z plane $\phi_{s0}(z)$ and $\psi_{s0}(z)$ must be bounded as $y \rightarrow \infty$ to insure that $\sigma_{ij}^{(s)}$ and $u_i^{(s)}$ are well behaved (Eq. (2)). Thus, in the z plane, if $\psi_{s0}(z)$ and $\phi_{s0}(z)$ are bounded, then in the t plane as $t \rightarrow 0$, $\Phi_{s0}(t)$ and $\Psi_{s0}(t)$ and also bounded.

In view of these considerations, we conclude that $u \ln u \Phi'_{\text{Re},s0}(u) \rightarrow 0$ as $u \rightarrow 0$. (Numerical calculations performed subsequently show that indeed $\Phi'_{\text{Re},s0}(0) = 0$.) This leads to the expression for the single-valued energy contribution, Eq. (62):

$$E_{\text{elas}}^{(s)}(\mu) = \left[\Psi_{\text{Re},s0}(u_0) + \Phi_{\text{Re},s0}(u_0) - 2u_0 \ln u_0 \Phi'_{\text{Re},s0}(u_0) \right] - \left[\Psi_{\text{Re},s0}(0) + \Phi_{\text{Re},s0}(0) \right]. \quad (65)$$

The solution to the integral equation, Eq. (52), yields $\Phi_{s0}(\tau)$ and hence $\Phi_{\text{Re},s0}(u_0)$, from which $\Psi_{\text{Re},s0}(u_0)$ and $\Phi'_{\text{Re},s0}(u_0)$ can be determined immediately. The boundary values of $\Phi_{s0}(\tau)$ and $\psi_{s0}(\tau)$ can then be used to calculate $\Psi_{\text{Re},s0}(0)$ and $\Phi_{\text{Re},s0}(0)$ by Cauchy's "outside" formula; thus

$$\Phi_{\text{Re},s0}(0) = \text{Re} \left[-\frac{1}{2\pi i} \int_L \frac{\Phi_{s0}(\tau)}{\tau} d\tau + \frac{1}{2\pi i} \int_L \frac{\Phi_{s0}(\tau)}{\tau - 1} d\tau \right] \quad (66)$$

and

$$\Psi_{\text{Re},s0}(0) = \text{Re} \left[-\frac{1}{2\pi i} \int_L \frac{\Psi_{s0}(\tau)}{\tau} d\tau + \frac{1}{2\pi i} \int_L \frac{\Psi_{s0}(\tau)}{\tau - 1} d\tau \right]. \quad (67)$$

Therefore, in principle, only the solution to Eq. (52) is required to determine the elastic energy completely.

The elastic energy may be recast into simpler form by examining Eqs. (62) and (63). Rewriting the form of these equations, we obtain

$$E_{\text{elas}}^{(m)}(\mu) = \frac{b}{2} [F_{\text{Re},m}(u_0) - F_{\text{Re},m}(\epsilon \rightarrow 0)] \quad (68)$$

and

$$E_{\text{elas}}^{(s)}(\mu) = \frac{b}{2} [F_{\text{Re},s}(u_0) - F_{\text{Re},s}(\epsilon \rightarrow 0)], \quad (69)$$

where $F_{\text{Re},\lambda}(u) = \Psi_{\text{Re},\lambda 0}(u) + \Phi_{\text{Re},\lambda 0}(u) - 2u \ln u \Phi'_{\text{Re},\lambda 0}(u)$, $\lambda = m$ or s , and $u = 0$ or u_0 . ($F_{\text{Re},\lambda}$ can be thought of as the shear force on the cut plane.)

Combining Eqs. (68) and (69), we obtain

$$E_{\text{elas}} = \frac{b}{2} [F_{\text{Re},m}(u_0) + F_{\text{Re},s}(u_0) - F_{\text{Re},m}(0) - F_{\text{Re},s}(0)] .$$

But $F_{\text{Re},m}(u_0) + F_{\text{Re},s}(u_0) = 0$ by the boundary conditions (as seen by examining Eq. (37)). Thus

$$E_{\text{elas}}(\mu) = \frac{h}{2} [F_{\text{Re},m}(0) + F_{\text{Re},s}(0)] ,$$

where $F_{\text{Re},m}(0) = E_0 \ln 4$ and $F_{\text{Re},s}(0) = \Phi_{\text{Re},s0}(0) + \Psi_{\text{Re},s0}(0)$, which yields

$$E_{\text{elas}}(\mu) = \frac{b}{2} [\Phi_{\text{Re},s0}(0) + \Psi_{\text{Re},s0}(0) + E_0 \ln 4] . \quad (70)$$

In this equation the terms $\Phi_{\text{Re},s0}(0)$ and $\Psi_{\text{Re},s0}(0)$ can be evaluated from Eqs. (66) and (67). It is reemphasized that the elastic energy is a function only of $\mu = r_0/h$.

The elastic interactions among the dislocations are entirely accounted by $E_{\text{elas}}^{(s)}(\mu)$, since the core boundary conditions are obeyed exactly. Let us first consider the dislocation at the origin (zeroth dislocation) when the dislocations are widely separated; $h \gg b$. The stresses from the adjacent dislocations acting on the core boundary of the zeroth dislocation would then be negligible. However, as h decreases, the contribution from adjacent dislocations eventually becomes substantial. Since the core boundary must remain traction free, the stresses $\sigma_{rr}^{(s)}$ and $\sigma_{r\xi}^{(s)}$ increase to cancel the growing contribution from adjacent dislocations. Hence $\sigma_{ij}^{(s)}$ includes the interaction from all other dislocations as well as the self-stress.

Numerical Solution

The integral equation, Eq. (52), can be solved for $\Phi_{s0}(\tau)$ only by numerical means, precluding any closed-form solution. Equation (52) becomes a system of two, real, coupled, Fredholm integral equations of the second kind when it is separated into its real and imaginary parts.

Equation (52) can be recast into an alternative form by parameterizing τ with respect to ξ , where ξ is the planar polar angle from the positive x axis in the z plane; this parameterization is given by Eq. (36). Letting

$$\Phi_{s0}[\tau(\xi)] = p(\xi) + iq(\xi) \quad (71)$$

and separating Eq. (52) into real and imaginary parts yields

$$p(\xi_0) + \mathcal{L} [K^A(\xi, \xi_0)p(\xi)] + \mathcal{L} [K^B(\xi, \xi_0)q(\xi)] = A^r(\xi_0) \quad (72)$$

and

$$-q(\xi_0) + \mathcal{L} [K^C(\xi, \xi_0)p(\xi)] + \mathcal{L} [K^D(\xi, \xi_0)q(\xi)] = A^i(\xi_0), \quad (73)$$

where

$$\mathcal{L}[\dots] = \int_0^{2\pi} (\dots) d\xi, \quad A^r(\xi_0) = \text{Re}[A(\xi_0)], \quad A^i(\xi_0) = \text{Im}[A(\xi_0)],$$

and $A(\xi_0)$ is given by Eq. (53).

The numerical solution to Eqs. (72) and (73) was obtained by approximating the integrals as a numerical quadrature (Simpson's rule was employed). The interval $\xi \in [0, 2\pi]$ was divided into $N + 1$ points, converting Eqs. (72) and (73) to a system of $2N + 2$ linearly independent equations, which may be written in matrix form as

$$\begin{bmatrix} K_{jk}^A w_k + \delta_{jk} & K_{jk}^B w_k \\ K_{jk}^C w_k & K_{jk}^D w_k - \delta_{jk} \end{bmatrix} \begin{pmatrix} p_j \\ q_j \end{pmatrix} = \begin{pmatrix} A_j^r \\ A_j^i \end{pmatrix}, \quad (74)$$

where the w_k terms are the weighting factors of the quadrature scheme.

A computer code was developed to calculate the kernels and to integrate $A(\xi_0)$ numerically. A standard matrix inversion code employing the Gauss elimination method was used to solve the $(2N + 2) \times (2N + 2)$ system of linear equations for p_j and q_j . Because of the symmetry of the kernels and $A(\xi_0)$, the limits of integration were reduced to a half range, permitting a finer point density of ξ to be used without exceeding machine capacity.

Values of p_j and q_j were calculated in intervals of $\Delta\xi = 2.25^\circ$ over $\xi \in [0, \pi]$ for many values of μ . For each μ calculation of $\sigma_{r\xi}$ at $r = r_0$ in the z plane was performed to check the results and verify the accuracy to which the boundary conditions are met. Excellent agreement was obtained for the cancellation of these stresses at $r = r_0$ as required by the boundary conditions. This led to high confidence of the numerically determined potentials $\Phi_{s0}(\tau)$ and $\Psi_{s0}(\tau)$, because the stresses were obtained from these potentials by numerical differentiation. Most numerical differentiation methods tend to magnify any error incurred in the calculation of the function.

From the numerically computed boundary values of $\Phi_{s0}(\tau)$ and $\Psi_{s0}(\tau)$, $E_{\text{elas}}^{(s)}$ was calculated from Eq. (65) in increments of $\Delta\mu = 0.025$ for $0 \leq \mu \leq 0.5$. (At $\mu = 0.5$, the cores impinge upon one another.) The resulting data were then fitted with a least-squares polynomial to yield

$$E_{\text{elas}}^{(s)}(\mu) = E_0 b \sum_{n=0}^7 a_n \mu^n, \quad (75)$$

where the coefficients a_n are listed in Table 1.

As a final check the total elastic energy was calculated two ways. Equation (75) was summed with Eq. (64), for the multivalued energy, to obtain values of the total elastic energy. These were then compared to the values obtained from Eq. (70), the simpler form for computing the total elastic energy. Both methods gave answers that were identical to six significant figures.

Table 1
Coefficients in the Expansion of

$$E_{\text{elas}}(\mu) = E_{\text{elas}}^{(m)}(\mu) + E_0 b \sum_{n=0}^7 a_n \mu^n, \text{ where}$$

$$E_{\text{elas}}^{(m)}(\mu) = E_0 b [\pi \mu \coth(\pi \mu) - \ln(2 \sinh \pi \mu)]$$

n	a_n
0	-0.49999
1	-0.00205
2	1.7178
3	-0.89875
4	0.95565
5	-9.7085
6	29.630
7	-28.344

The total elastic energy per strip of grain boundary, Eq. (70), is shown as a function of μ in Fig. 7, along with the results of Refs. 3 and 14. The present exact analysis and that of Glicksman and Vold are indistinguishable for $\mu < 0.3$. However, the treatment by Glicksman and Vold eventually leads to negative energies at $\mu \gtrsim 0.4$, because in their approximate analysis the boundary conditions at the dislocation cores are violated (that is, the grain-boundary dislocation cores near $\mu = 0.5$ no longer remain traction free). The present analysis yields an elastic energy that is always positive definite and approaches zero as μ approaches 0.5. When $\mu = 0.5$, the cores impinge upon one another and crystals 1 and 2 (Fig. 1) are then joined continuously by the "core" phase, which according to our model cannot store any elastic energy, because all stress components are zero; thus $E_{\text{elas}}(0.5)$ must be zero. In contrast to the present theory and that of Glicksman and Vold, the Read and Shockley treatment (Eq. (64)) yields an elastic energy which is always larger, because no interactions are taken into account. A critical aspect of the present theory is the detailed behavior of $E_{\text{elas}}(\mu)$ as $\mu \rightarrow 0.5$, since the derivative $\partial E_{\text{elas}}/\partial \mu$ will be used subsequently to calculate the total grain-boundary energy.

CORE ENERGY

At temperatures near or at the melting point of the solid, dislocation cores are considered here to behave as a liquidlike second phase. The chemical (nonelastic) energy of an individual core can be written in a phenomenological form as

$$E_{\text{chem}}(r_0) = 2\pi\gamma_c r_0, \quad (76)$$

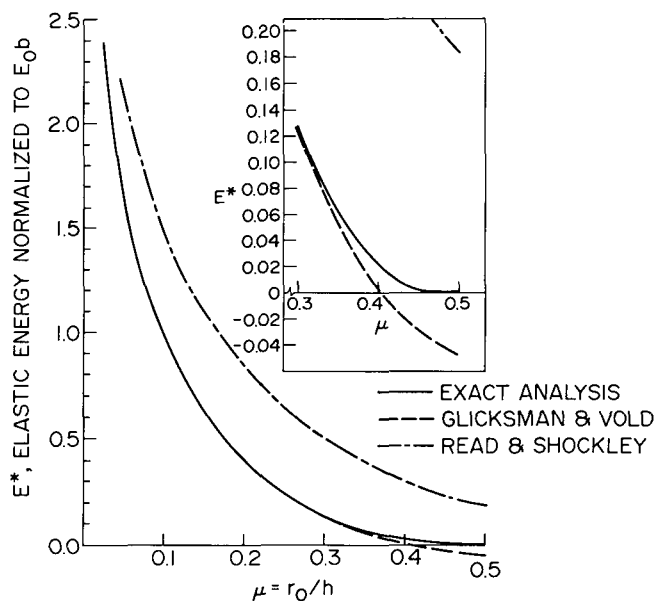


Fig. 7—Comparison of the normalized elastic energy as a function of μ obtained from Eq. (70) (equivalent to the sum of Eqs. (75) and (64)) with that from Ref. 3 and from Ref. 14. The insert is an expanded portion of the plot for $0.3 \leq \mu \leq 0.5$.

where r_0 is the radius of the core and γ_c is the specific free-energy of the core per unit area of core-crystal “interface.” Equation (76) may be rewritten slightly in a form compatible with the previous elastic-energy analysis, namely,

$$E_{\text{chem}}(\mu) = 2\pi\gamma_c\lambda\mu. \quad (77)$$

GRAIN-BOUNDARY ENERGY

The total free energy of the system is the sum of the chemical and elastic energies,

$$E_t(\mu) = E_{\text{chem}}(\mu) + E_{\text{elas}}(\mu), \quad (78)$$

where $E_{\text{chem}}(\mu)$ is given by Eq. (77) and $E_{\text{elas}}(\mu)$ is obtained from the sum of Eqs. (64) and (75). The only remaining “free” geometric parameter which can vary in our model is r_0 , the core radius; thus for thermodynamic equilibrium we seek

$$\frac{\partial E_t}{\partial r_0} = \frac{1}{h} \frac{\partial E_t}{\partial \mu} = 0$$

or

$$\frac{\partial E_t}{\partial \mu} = 0 = \kappa + \sum_{n=0}^7 na_n\mu^{n-1} - \pi^2\mu \coth^2 \pi\mu, \quad (79)$$

where h is fixed, $\kappa = \lambda/\theta$, $\lambda = 2\pi\gamma_c/E_0$, and $\theta = b/h$ (from Eq. (30)).

For a given κ the value of $\mu = \mu^*$ which satisfies Eq. (79) was determined numerically by the "regula falsi" technique [24]. Figure 8 is a plot of μ^* for $0 \leq \kappa \leq 24$. In that figure μ^* decreases monotonically from a maximum value of 0.5 as κ increases.

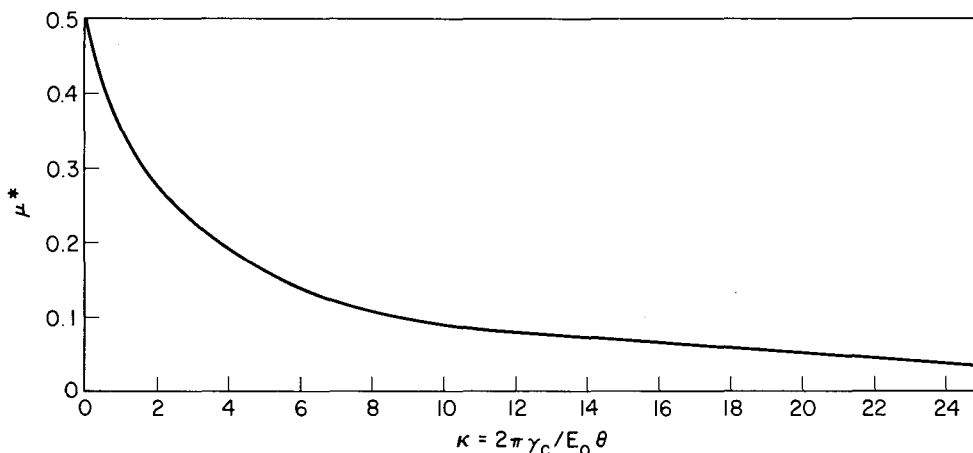


Fig. 8—Normalized equilibrium radius $\mu^* = r_0^*/h$ vs $\kappa = \lambda/\theta = 2\pi\gamma_c/\theta E_0$

The solution to Eq. (79) yields $\mu^* = f(\kappa)$, and when this is inserted into Eq. (78), the minimum free energy of the grain boundary system is obtained. The energy per unit area of grain boundary is then

$$\Gamma_B = E_t(\mu^*)/h. \quad (80)$$

Normalizing Eq. (80) with respect to $E_0\theta$ yields

$$\frac{1}{\theta} \frac{\Gamma_B}{E_0} = \kappa\mu^* + \sum_{n=0}^7 a_n(\mu^*)^n + \pi\mu^* \coth \pi\mu^* - \ln(2 \sinh \pi\mu^*). \quad (81)$$

This equation contains only one material parameter κ , which is the ratio of two phenomenological quantities γ_c and E_0 —reflecting the elasto-chemical nature of this theory.

A "master curve" of the normalized grain-boundary energy was obtained by plotting Eq. (81) as a function of κ as shown in Fig. 9. From this plot, the grain boundary energy Γ_B , vs tilt misorientation, θ can be deduced for a given γ_c and E_0 . The chemical and elastic contributions to the grain boundary energy can easily be determined.

The sensitivity of Γ_B with varying λ is illustrated in Fig. 10. For $\lambda = 5$ the elastic energy is always larger than the chemical contribution. At this large value of λ equilibrium demands a small value of r_0 , since γ_c is rather large compared to E_0 ; hence the E_{chem} contribution is small relative to E_{elas} . However at $\lambda = 0.5$ the opposite behavior is noted. In this case the elastic energy reaches a broad maximum and decreases slowly with increasing misorientation. The curves for $\lambda = 0.5$ are similar to those of van der Merwe [5]. In spite of the differing behavior for the two values of λ used, one distinct conclusion may be drawn: The elastic energy always dominates over the chemical energy contribution from the cores when $\theta < 1^\circ$, that is, when the dislocations are widely separated ($h > 60b$).

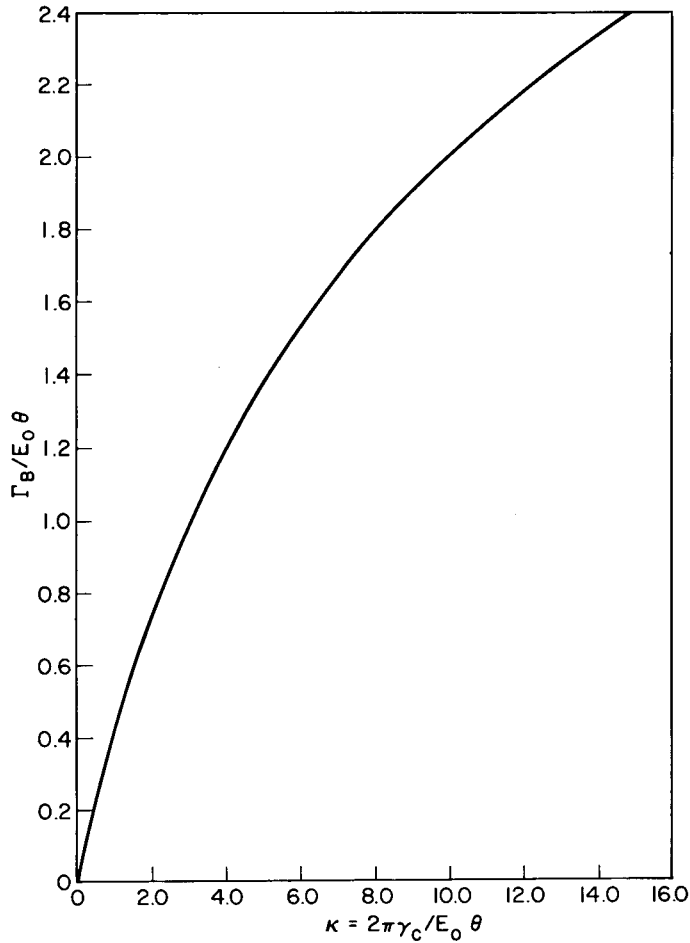


Fig. 9—"Master plot" of the normalized grain-boundary energy. For given E_0 , γ_c , and θ , κ can be computed and, Γ_B using Eq. (81), $\Gamma_B/E_0\theta$ can be determined.

For small tilt misorientations the dislocations are widely separated ($\mu \rightarrow 0$) and the interaction effects become negligible. As $\mu \rightarrow 0$ the elastic energies reduce to

$$E_{\text{elas}}^{(m)} \rightarrow E_0 b (1 - \ln 2\pi\mu) \quad (82)$$

and

$$E_{\text{elas}}^{(m)} \rightarrow -E_0 b / 2. \quad (83)$$

Equation (82) can be manipulated to yield the low-angle Read-Shockley (RS) formula [3,4]

$$\Gamma_{\text{BRS}} = E_0\theta [A_{\text{RS}} - \ln \theta],$$

by using the relation $\mu = (r_0/b)\theta$ and by choosing

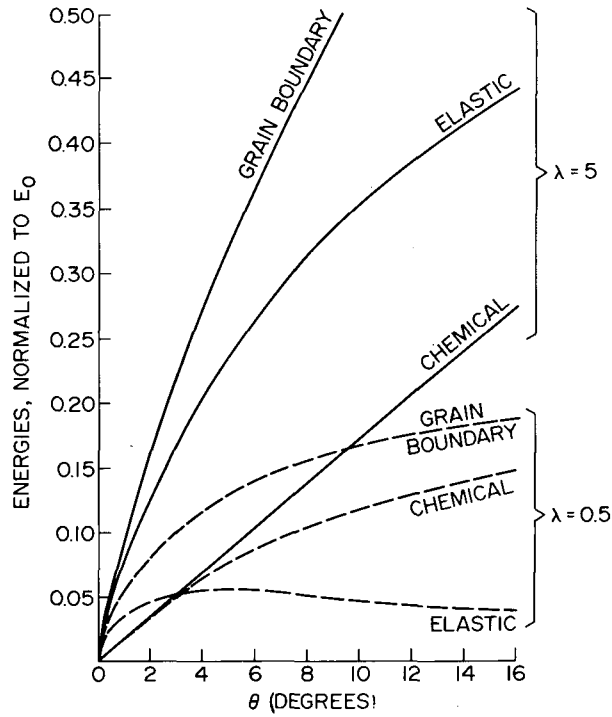


Fig. 10—Elastic, chemical, and total grain-boundary energies as a function of tilt misorientation θ , indicating the sensitivity of these energies on the parameter $\lambda = 2\pi\gamma_c/E_0$

$$A_{RS} = 1 - \ln \frac{2\pi r_0}{b}. \quad (84)$$

The Read-Shockley formulation does not account for boundary conditions at each dislocation core.

In this low-angle regime the heterophase dislocation model with equilibrated cores yields an A constant different from the Read-Shockley case. At these small misorientations the present theory reduces identically to the formulation of Glicksman and Vold [14]. The total free energy of the system is the sum of Eqs. (77), (82), and (83):

$$E_t(\mu) = 2\pi\gamma_c\mu h + E_0 b \left(\frac{1}{2}\right) - \ln 2\pi\mu$$

or

$$E_t(r_0) = 2\pi\gamma_c r_0 + E_0 b \left(\frac{1}{2}\right) - \ln 2\pi \frac{r_0}{h}. \quad (85)$$

Again, for equilibrium we set $\partial E_t/\partial r_0 = 0$, which leads to

$$r_0 = \frac{E_0 b}{2\pi\gamma_c}. \quad (86)$$

Inserting Eq. (86) into Eq. (85) and using the definition of the grain boundary energy, Eq. (80), leads to the formula derived by Glicksman and Vold (GV)

$$\Gamma_{BGV} = E_0 \theta (A_{GV} - \ln \theta), \quad (87)$$

where

$$A_{GV} = \frac{3}{2} - \ln \frac{2\pi r_0}{b}. \quad (88)$$

Equations (84) and (88) differ by $1/2$, which is the effect of the equilibrated core condition as reflected through $E_{elas}^{(s)}$, Eq. (83).

APPLICATION TO EXPERIMENT

In Fig. 11 are shown experimental grain-boundary-energy data [25,26] for $\{\bar{1}\bar{1}0\}$ tilt boundaries in bismuth near its melting point. Also shown in that figure are results from the theory of Read and Shockley and from the present theory, Eq. (80). The Read and Shockley theory, being in a sense nonpredictive, required the theoretical curve to be fitted at low tilt misorientations to evaluate the unknown parameter ($r_0/b = 1.15$). This theory yields a maximum in the energy occurring around $\theta = 8^\circ$, whereas the experimental data clearly indicate a gradual and continuous upward trend. For the present theory the best fit through the *entire* set of experimental data was accomplished with the value $\lambda = 0.45$. At this value of λ the ratio $\gamma_c/\gamma_{sl} \approx 0.8$, which supports the hypothesis that the core material resembles to some extent the liquid phase at high temperatures. Since $\gamma_c \approx \gamma_{sl}$, one could use as a first approximation a value of $\lambda = 2\gamma_{sl}/E_0$ to estimate a priori the grain boundary energy in materials near their melting point.

In contrast to the Read and Shockley theory, where r_0/b is fixed, the r_0/b calculated from this theory is a function of θ and varies from about $r_0/b = 2.25$ at $\theta \ll 1^\circ$ to $r_0/b = 1.4$ at $\theta \approx 15^\circ$. This result indicates that it might be difficult to extend an elasto-chemical theory to larger tilt misorientations, since it would be tenuous to ascribe thermodynamic properties to dislocation cores containing just a few atoms.

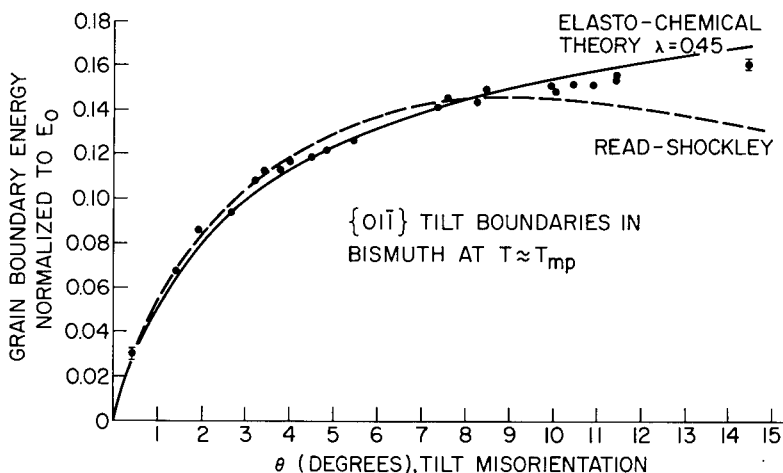


Fig. 11—Comparison of experimental data points for bismuth [25,26] with theory

The data of Fig. 11 are replotted in Fig. 12 as a function of $\Gamma_B/\theta E_0$. The present theory ($\lambda = 0.45$) is the solid line, which is linear (slope = -1.0) for small θ (Eq. (87)), and the dashed line is the extension of this linear region. The salient feature of this result is that the deviation from linearity occurs at $\theta \gtrsim 2.0^\circ$. This means that extremely-low-angle grain-boundary-energy data ($\theta < 2.0^\circ$) must be used to determine the A constant correctly. By contrast, when a "best fit" linear segment was fitted through the experimental data points for bismuth in Fig. 12, this line (dashed-dotted line) is shifted to the right, yielding a smaller (erroneous) value of A and hence a smaller r_0/b . Thus extremely-low-angle grain-boundary-energy data are essential, as pointed out earlier by Gjostein [27], and as a consequence the approximate formulas have a severely limited range of validity (less than 2° of tilt misorientation in the case of bismuth).

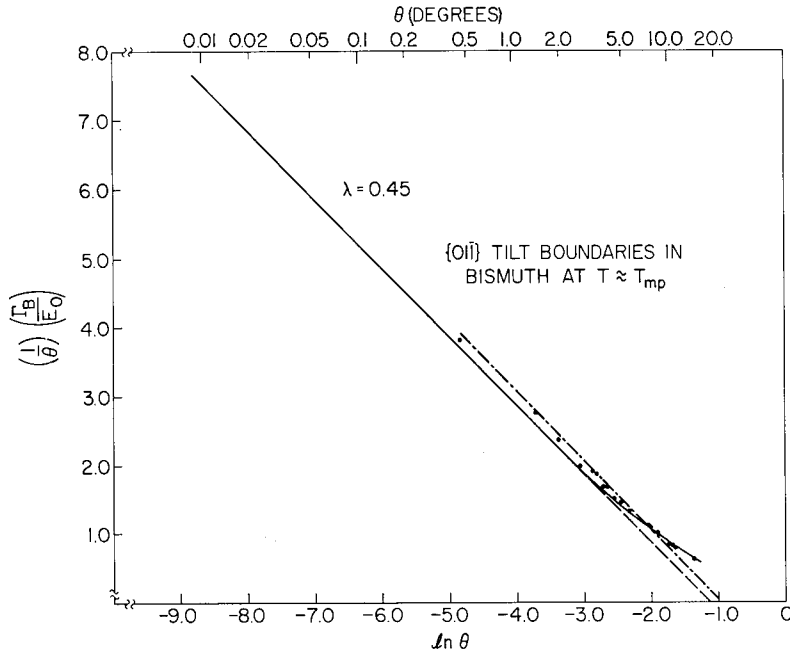


Fig. 12—Normalized grain-boundary-energy as a function of $\ln \theta$. The solid line is the present theory, and the dashed line is the extension of the linear region. The dashed-dotted line is the best fit through experimental data points.

SUMMARY

In summary:

- The theory of heterophase dislocations provides a thermodynamic basis for determining absolute grain-boundary energies at temperatures near the melting point. The concept of a liquidlike dislocation core was proven to be a valid approximation for bismuth, since $\gamma_c \approx \gamma_{sl}$.
- A major aspect of this theory is the inclusion of elastic interactions among dislocations. This leads to a formulation of grain boundary energetics in terms of the core-crystal energy and the elastic moduli, which are estimable phenomenological parameters.

- The elastic energy contribution dominates over the chemical (or core) contribution only for boundaries with tilt misorientations less than about 1° , where the dislocations are spaced more than about $60b$ apart.

- If the assumption, $\gamma_c \approx \gamma_{sl}$, is made, the theory provides a first estimate of the excess grain-boundary free energy, when interfacial free energies and elastic moduli are known independently. Entropic contributions to the grain-boundary free energy arising both from the elastic and core contributions are entirely accounted for with this thermodynamic formulation.

- The tendency for the dislocation core radius to shrink as the dislocations approach each other imposes a limit on the validity of the model at large tilt misorientations. Specifically, an upper limit of approximately 10° to 15° is found for typically metallic cases, where the core radius falls to about one Burgers vector. At smaller tilt misorientations, where the cores are larger (2 to 3 Burgers vectors in radius), the thermodynamic treatment appears to be on firmer ground.

- The application of the low-angle formulas requires extremely-low-angle experimental grain-boundary-energy data ($\theta < 2^\circ$). Thus these formulas are valid only over a limited range of tilt misorientation, much smaller than recognized heretofore.

- The present model uses continuum concepts throughout, and lattice geometrical effects such as coincidence site boundaries are excluded from consideration. The present theory should best be thought as accounting for rotations between crystals arising from localized elastic strain centers which may interact with each other through the short-range elastic fields surrounding the boundary. The rotations arising from the elastic distortions may be thought of as providing a relatively wide and continuous range (up to $\pm 15^\circ$) of tilt misorientations about any strong lattice coincidence.

- Despite the finite rotations of the adjacent crystals, no ambiguity arises in the definition of the Burgers vector for the boundary dislocations. The Burgers vector always remains normal to the boundary (for tilt boundaries, as considered in this report) and is of magnitude θh . As a practical matter the product θh will *appear* to remain constant and, to within experimental precision, will *appear* to be the magnitude of a small lattice vector. However, the theory as developed here imposes no requirement that the Burgers vector of a grain boundary dislocation be a (strain-free) lattice vector, and it is the confusion over the point that leads to an apparent ambiguity.

REFERENCES

1. G.I. Taylor, *Proc. Royal Soc. London* 145A, 362 (1934).
2. J.M. Burgers, *Proc. Kon. Ned. Akad. Wet.* 42, 293 (1939).
3. W.T. Read and W. Shockley, *Phys. Rev.* 78, 275 (1950).
4. W.T. Read, *Dislocations in Crystals*, New York, McGraw-Hill, 1953, Ch. 11.
5. J.H. van der Merwe, *Proc. Phys. Soc.* 63A, 616 (1950).
6. N.H. Fletcher and P.L. Adamson, *Phil. Mag.* 14, 99 (1966).
7. G. Hasson and C. Goux, *Compte Rendu* 271C, 1048 (1970).
8. S. Ranganathan, *Acta Cryst.* 21, 197 (1966).

9. D.G. Brandon, *Acta Met.* **14**, 1479 (1966).
10. W. Bollmann, *Phil. Mag.* **16**, 363 (1967).
11. G.H. Bishop and B. Chalmers, *Phil. Mag.* **24**, 515 (1971).
12. T. Schober and R.W. Balluffi, *Phys. Stat. Sol. (b)* **44**, 115 (1971).
13. J.C.M. Li, *J. App. Phys.* **32**, 525 (1961).
14. M.E. Glicksman and C.L. Vold, *Surface Science* **31**, 50 (1972).
15. N.I. Muskhelishvili, *Some Basic Problems of the Mathematical Theory of Elasticity*, Groningen, Noorhoff, 1953, pp. 104-155.
16. S.G. Mikhlin, *Integral Equations*, New York, Pergamon Press, 1957, pp. 250-255.
17. R.C.J. Howland, *Proc. Roy. Soc. London* **148A**, 471 (1935).
18. K.J. Schulz, *Proc. Kon. Ned. Akad. Wet.* **45**, 233 (1942).
19. J.P. Hirth and J. Lothe, *Theory of Dislocations*, New York, McGraw-Hill, 1968, p. 670.
20. F.R.N. Nabarro, *Theory of Crystal Dislocations*, Oxford, Clarendon, 1967, pp. 30-37.
21. G.N. Savine, *Doklady ANSSSR (Comptes Rendus de l'Academie des Sciences de l'U.R.S.S.)* **23**, 515 (1939).
22. D.I. Sherman, *Trudy Seismological Inst. ANSSSR* **86**, 1 (1938).
23. I.S. Sokolnikoff, *Mathematical Theory of Elasticity*, 2nd edition, New York, McGraw-Hill, 1956, p. 86.
24. F.B. Hildebrand, *Introduction to Numerical Analysis*, New York, McGraw-Hill, 1956, p. 446.
25. M.E. Glicksman and C.L. Vold, *Acta Met.* **17**, 1 (1969).
26. M.E. Glicksman and C.L. Vold, *Scripta Met.* **5**, 493 (1971).
27. N.A. Gjostein, *Acta Met.* **8**, 263 (1960).

Appendix A

EVALUATION OF THE COMPLEX CONSTANTS α AND β

In this appendix, we evaluate the complex constants, α and β , which appear in the expressions for the complex potentials, Eqs. (17) and (18), namely,

$$\phi_{m0}(z) = \alpha \ln \sin \frac{\pi z}{h} \quad (\text{A1})$$

and

$$\psi_{m0}(z) = \beta \ln \sin \frac{\pi z}{h}. \quad (\text{A2})$$

These constants are evaluated from the multivalued displacements and zero-resultant force conditions.

The displacements are given in Eq. (11) in terms of the complex potentials. When Eqs. (A1) and (A2) are substituted into Eq. (11), we have

$$2G \left[u_x^{(m)} + iu_y^{(m)} \right] \Big|_A^B = \left(\alpha K \ln \sin \frac{\pi z}{h} - 2iy \frac{\pi}{h} \bar{\alpha} \cot \frac{\pi z}{h} - \bar{\beta} \ln \sin \frac{\pi z}{h} \right) \Big|_A^B, \quad (\text{A3})$$

where A and B are the endpoints of an arc.

Expanding $\sin \pi z/h$ as

$$\sin \frac{\pi z}{h} = A e^{i\gamma}, \quad (\text{A4})$$

and letting $\eta = \pi x/h$ and $\omega = \pi y/h$, we find that

$$A^2 = \sin^2 \eta + \sinh^2 \omega \quad (\text{A5})$$

and

$$\tan \gamma = \frac{(\cos \eta)(\sinh \omega)}{(\sin \eta)(\cosh \omega)}. \quad (\text{A6})$$

By substituting Eq. (A4) and using the relationship

$$\cot \zeta = \frac{\sin 2\eta - i \sinh 2\omega}{\cosh 2\zeta - \cos 2\omega}, \quad (\text{A7})$$

where

$$\zeta = \frac{\pi}{h} z = \frac{\pi}{h} (x + iy), \quad (\text{A8})$$

Eq. (A3) becomes

$$2G \left[u_x^{(m)} + iu_y^{(m)} \right] \Big|_A^B = \left[\ln A(K\alpha - \bar{\beta}) + i\gamma(\alpha K + \bar{\beta}) - 2i\bar{\alpha}\omega \frac{\sin 2\eta + i \sinh 2\omega}{\cosh 2\omega - \cos 2\eta} \right] \Big|_A^B. \quad (\text{A9})$$

In particular let A and B be the endpoints of an arc (or contour when in the complex plane) L_0 which encloses one dislocation (for convenience the one at the origin) and such that $y_A = y_B$ (Fig. 2 of the main text). Mathematically a branch cut is made along the y axis to render the displacements single valued. Thus the polar angle ξ is defined for $-3/2\pi \leq \xi \leq \pi/2$. The prescribed displacements on the branch cuts are as follows:

$$\left. \begin{array}{l} \text{right branch:} \\ \text{left branch:} \end{array} \right\} \begin{array}{ccc} \xi & u_x & u_y \\ \hline \pi/2 & 0 & b \\ -3/2\pi & 0 & 0 \end{array}, \quad r \geq r_0,$$

where b is the magnitude of the grain boundary Burgers vector. Thus

$$\left[u_x^{(m)} + iu_y^{(m)} \right] \Big|_{L_0} = ib. \quad (\text{A10})$$

When the right-hand side of Eq. (A9) is evaluated around L_0 , the only term which is not zero is

$$i(\alpha K + \bar{\beta})\gamma \Big|_{L_0} \neq 0.$$

Thus

$$2iGb = i(\alpha K + \bar{\beta})\gamma \Big|_{L_0}. \quad (\text{A11})$$

To evaluate $\gamma|_{L_0}$, consider the mapping

$$y' = \cos \eta \sinh \omega$$

and

$$x' = \sin \eta \cosh \omega,$$

where $z' = x' + iy'$, so that

$$\gamma \Big|_{L_0} = \tan^{-1} \frac{\cos \eta \sinh \omega}{\sin \eta \cosh \omega} \Big|_{L_0} = \tan^{-1} \frac{y'}{x'} \Big|_{L'_0},$$

and where L'_0 is L_0 mapped into the z' plane. In the z' plane,

$$\tan^{-1} \frac{y'}{x'} \Big|_{L'_0} = 2\pi ;$$

hence

$$\gamma|_{L_0} = 2\pi . \tag{A12}$$

Thus from Eqs. (A11) and (A12),

$$\alpha K + \bar{\beta} = \frac{Gb}{\pi} .$$

The resultant force acting on the dislocation must be equal to zero for equilibrium. Thus inserting Eqs. (A1) and (A2) into Eq. (12), we must have

$$\left(\alpha \ln \sin \frac{\pi z}{h} + \bar{\beta} \overline{\ln \sin \frac{\pi z}{h}} + 2iy \frac{\pi}{h} \bar{\alpha} \overline{\cot \frac{\pi z}{h}} \right) \Big|_{L_0} = 0 . \tag{A13}$$

Using the previous results we find that

$$(\alpha - \bar{\beta})\gamma|_{L_0} = 0 .$$

But $\gamma|_{L_0} = 2\pi$; hence

$$\alpha = \bar{\beta} .$$

The constants α and β can be individually determined from Eqs. (A13) and (A12) to yield

$$\alpha = \beta = \frac{Gb}{4\pi(1-\nu)} ,$$

which is a real constant.

Appendix B

ELASTIC FIELD OF A SINGLE ISOLATED EDGE DISLOCATION OBTAINED BY LETTING THE EDGE-DISLOCATION SPACING APPROACH INFINITY IN THE PERIODIC CASE

In this appendix σ_{ij} and u_i arising from the discontinuity in displacement for the isolated case may be recovered from the periodic elastic fields by letting $h \rightarrow \infty$. In this limit these field quantities are the same as those often developed in many texts on the theory of dislocations.

First we consider the Cartesian stress components $\sigma_{xx}^{(m)}$, $\sigma_{yy}^{(m)}$, and $\sigma_{xy}^{(m)}$. From Eqs. (25) through (27)

$$\sigma_{xy}^{(m)} = \sigma_0(2\omega)(1 - \cos 2\eta \cosh 2\omega), \quad (\text{B1})$$

$$\sigma_{xx}^{(m)} = \sigma_0 \sin 2\eta (\cosh 2\omega - \cos 2\eta - 2\omega \sinh 2\omega), \quad (\text{B2})$$

and

$$\sigma_{yy}^{(m)} = \sigma_0 \sin 2\eta (\cosh 2\omega - \cos 2\eta + 2\omega \sinh 2\omega), \quad (\text{B3})$$

where $\sigma_0 = 2E_0(\pi/h)/(\cosh 2\omega - \cos 2\eta)^2$, $\omega = \pi y/h$ and $\eta = \pi x/h$. We let $h \rightarrow \infty$; then

$$\sigma_0 \rightarrow \frac{E_0}{2} \left(\frac{\pi}{h}\right)^3 r^4, \quad r^2 = x^2 + y^2, \quad (\text{B4})$$

$$1 - \cosh 2\omega \cos 2\eta \rightarrow 2 \left(\frac{\pi}{h}\right)^2 (y^2 - x^2), \quad (\text{B5})$$

$$\cosh 2\omega \cos 2\eta \rightarrow 2 \left(\frac{\pi}{h}\right)^2 r^2, \quad (\text{B6})$$

and

$$2\omega \sinh 2\omega \rightarrow 4 \left(\frac{\pi}{h}\right)^2 y^2. \quad (\text{B7})$$

Thus

$$\sigma_{xy}^{(m)} \rightarrow \frac{2E_0}{r^4} y(y^2 - x^2), \quad (\text{B8})$$

$$\sigma_{xx}^{(m)} \rightarrow \frac{2E_0}{r^4} x(x^2 - y^2), \quad (\text{B9})$$

and

$$\sigma_{yy}^{(m)} \rightarrow \frac{2E_0}{r^4} x(x^2 + 3y^2). \quad (\text{B10})$$

The displacement components u_x and u_y , Eqs. (28) and (29), become in the limit as $h \rightarrow \infty$

$$u_x^{(m)} \rightarrow \frac{E_0}{2G} \left[\frac{(K-1)}{2} \ln r^2 + \frac{2y^2}{r^2} \right] \quad (\text{B11})$$

and

$$u_y^{(m)} \rightarrow \frac{E_0}{2G} \left[(K+1) \tan^{-1} \frac{y}{x} - \frac{2xy}{r^2} \right], \quad (\text{B12})$$

where $E_0 = Gb/4\pi(1-\nu)$ and $K = 3 - 4\nu$.

To convert Eqs. (B8) through (B12) into the coordinate system that is commonly used in the various texts, where the slip plane is horizontal, a rotation of $\pi/2$ is required, namely, $x' = y$ and $y' = -x$. Under this rotation the stresses become

$$\sigma_{x'x'}^{(m)} = \sigma_{yy}^{(m)} = -\sigma'_0 y' \left[3(x')^2 + (y')^2 \right], \quad (\text{B13})$$

$$\sigma_{y'y'}^{(m)} = \sigma_{xx}^{(m)} = \sigma'_0 y' \left[(x')^2 - (y')^2 \right], \quad (\text{B14})$$

and

$$\sigma_{x'y'}^{(m)} = -\sigma_{xy}^{(m)} = \sigma'_0(x') \left[(x')^2 - (y')^2 \right], \quad (\text{B15})$$

where

$$\sigma'_0 = \frac{2E_0}{[(x')^2 + (y')^2]^2}.$$

The displacement components after rotation of $\pi/2$ are

$$u'_x = u_y = \frac{b}{2\pi} \left\{ \tan^{-1} \frac{y'}{x'} + \frac{x'y'}{[2(1-\nu)(x')^2 + (y')^2]} - \frac{\pi}{2} \right\}, \quad (\text{B16})$$

and

$$u'_y = -u_x = -\frac{b}{2\pi} \frac{1}{4(1-\nu)} \left\{ \ln \left[(x')^2 + (y')^2 \right] + \frac{(x')^2 - (y')^2}{(x')^2 + (y')^2} + 1 \right\}. \quad (\text{B17})$$

Since the last terms appearing on the right-hand sides of Eqs. (B16) and (B17) are rigid-body displacements, they do not affect the strain and stress distribution and may therefore be neglected. Equations (B13) through (B17) are in agreement with those of Hirth and Lothe [19, pp. 74-75].

Appendix C

AN INTEGRAL-EQUATION APPROACH TO THE SINGLE ISOLATED EDGE DISLOCATION WITH AN EQUILIBRATED CORE

When $\mu \rightarrow 0$ (the ratio of the core radius to dislocation spacing approaches zero), each dislocation acts as if it were isolated in an infinite medium. In this limit $\mu \rightarrow 0$, the periodicity effects are negligible and the appropriate multivalued potentials are given by Eqs. (7) and (8) of the main text, namely,

$$\phi_m(z) = \phi_{m0}(z) = E_0 \left[\ln z + \ln \frac{\pi}{h} \right] \quad (C1)$$

and

$$\psi_m(z) = \psi_{m0}(z) - z\phi'_{m0}(z) = E_0 \left[\ln z + \ln \frac{\pi}{h} - 1 \right]. \quad (C2)$$

The equilibrated core conditions, $\sigma_{rr} = 0$ and $\sigma_{r\xi} = 0$ at $r = r_0$, are inserted into the force balance to yield

$$\phi_s(\bar{z}) = \overline{\bar{z}\phi'_s(\bar{z})} + \overline{\psi_s(\bar{z})} = f_m(\bar{z}), \quad (C3)$$

where \bar{z} is any point on the circular core boundary $\bar{z} = r_0 e^{i\xi}$, ξ is the polar angle defined from the x axis, and $f_m(\bar{z})$ is given as

$$f_m(\bar{z}) = - \left[\phi_m(\bar{z}) + \overline{\bar{z}\phi'_m(\bar{z})} + \overline{\psi_m(\bar{z})} \right]$$

or

$$f_m(\bar{z}) = -E_0 \left[2 \ln \pi \mu - 1 + \left(\frac{\bar{z}}{r_0} \right)^2 \right], \quad \mu = \frac{r_0}{h}. \quad (C4)$$

The solution to Eq. (C4) yields $\phi_s(\bar{z})$ and $\psi_s(\bar{z})$, from which the "single-valued" elastic fields can be determined.

In a similar fashion as in the periodic case, Eq. (C4) is converted into an integral equation,

$$\frac{1}{2} \phi_s(\bar{z}_0) + \frac{1}{2\pi i} \int \frac{\phi_s(\bar{z})}{\bar{z} - \bar{z}_0} d\bar{z} + \frac{1}{2} \overline{\bar{z}_0 \phi'_s(\bar{z}_0)} + \frac{1}{2\pi i} \int \frac{\overline{\bar{z}\phi'_s(\bar{z})}}{\bar{z} - \bar{z}_0} d\bar{z} = A(\bar{z}_0), \quad (C5)$$

where \bar{z}_0 is a point on the core boundary and

$$A(z_0) = \frac{1}{2} \overline{f_m(z_0)} + \frac{1}{2\pi i} \int \frac{\overline{f_m(z)}}{z - z_0} dz. \quad (C6)$$

The term $A(z_0)$ can be evaluated from Eq. (C4) to yield

$$A(z_0) = -E_0(2 \ln \pi\mu - 1), \quad (C7)$$

which is a real constant.

In view of the simple form for $A(z_0)$, the integral Eq. (C5) does not have to be reduced to the Fredholm form. Since $A(z_0)$ is a real constant, it suggests that a solution of the form

$$\phi_s(z) = \alpha, \quad (C8)$$

which is a real constant, will satisfy Eq. (C6). Inserting Eqs. (C8) into (C6) yields

$$\frac{1}{2} \alpha + \frac{1}{2\pi i} \alpha \int \frac{dz}{z - z_0} = -E_0(2 \ln \pi\mu - 1). \quad (C9)$$

But $\int (dz/(z - z_0)) = i\pi$; hence

$$\alpha = -E_0(2 \ln \pi\mu - 1), \quad (C10)$$

and from Eq. (C8)

$$\phi_s(z) = \alpha = -E_0(2 \ln \pi\mu - 1). \quad (C11)$$

Applying Cauchy's "outside" formula, for a point z in the elastic medium, we find $\phi_s(z)$ and $\psi_s(z)$ as

$$\psi_s(z) = -E_0 \left(\frac{r_0}{z} \right)^2 \quad (C12)$$

and

$$\phi_s(z) = -E_0(2 \ln \pi\mu - 1). \quad (C13)$$

The stresses σ_{rr} and $\sigma_{r\xi}$ can be calculated from the results of Muskhelishvili [15, p. 138], namely,

$$\sigma_{rr} - i\sigma_{r\xi} = 2 \operatorname{Re} [\phi'(z)] - e^{2i\xi} [\bar{z}\phi''(z) + 4'(z)],$$

where $\phi(z) = \phi_s(z) + \phi_m(z)$ and $\psi(z) = \psi_s(z) + \psi_m(z)$. Thus

$$\sigma_{rr} - i\sigma_{r\xi} = \frac{2E_0}{r_0} \left[1 - \left(\frac{r_0}{r} \right)^2 \right] e^{-i\xi};$$

and if $r = r_0$, then $\sigma_{rr} = \sigma_{r\xi} = 0$ and the boundary conditions are satisfied.

